Published for SISSA by Springer

Received: *September 18, 2017*
Accepted: *October 19, 2017*
Published: *October 26, 2017*

Towards next-to-next-to-leading-log accuracy for the width difference in the $B_s - \bar{B}_s$ system: fermionic contributions to order $(m_c/m_b)^0$ and $(m_c/m_b)^1$

H.M. Asatrian,[a] **A. Hovhannisyan,**[a] **U. Nierste**[b] **and A. Yeghiazaryan**[a]

[a] *Yerevan Physics Institute, Alikhanian Br. 2, 0036 Yerevan, Armenia*

[b] *Institut für Theoretische Teilchenphysik, Karlsruhe Institute of Technology, Engesserstraße 7, 76128 Karlsruhe, Germany*

E-mail: hrachia@yerphi.am, artyom@yerphi.am, ulrich.nierste@kit.edu, arseny@yerphi.am

Abstract: We calculate a class of three-loop Feynman diagrams which contribute to the next-to-next-to-leading logarithmic approximation for the width difference $\Delta\Gamma_s$ in the $B_s - \bar{B}_s$ system. The considered diagrams contain a closed fermion loop in a gluon propagator and constitute the order $\alpha_s^2 N_f$, where N_f is the number of light quarks. Our results entail a considerable correction in that order, if $\Delta\Gamma_s$ is expressed in terms of the pole mass of the bottom quark. If the $\overline{\text{MS}}$ scheme is used instead, the correction is much smaller. As a result, we find a decrease of the scheme dependence. Our result also indicates that the usually quoted value of the NLO renormalization scale dependence underestimates the perturbative error.

Keywords: NLO Computations

ArXiv ePrint: 1709.02160

https://doi.org/10.1007/JHEP10(2017)191

JHEP10(2017)191

Contents

1 Introduction

$B_s - \bar{B}_s$ oscillations are governed by the 2×2 matrix $M - i\Gamma/2$, which contains the mass matrix $M = M^\dagger$ and the decay matrix $\Gamma = \Gamma^\dagger$. By diagonalising $M - i\Gamma/2$ one finds the mass eigenstates B_L and B_H with the subscripts denoting "light" and "heavy", respectively. The eigenvalues $M_L - i\Gamma_L/2$ and $M_H - i\Gamma_H/2$ define masses and decay width of B_L and B_H. The time-dependent states $B_L(t)$ and $B_H(t)$ each obey exponential decay laws with decay constants Γ_L and Γ_H. By transforming back to the flavour basis $(B_s, \bar{B}_s)$ one finds the familiar damped oscillations between these flavour eigenstates. The mixing problem involves five observables:

$$M = \frac{M_L + M_H}{2}, \quad \Gamma = \frac{\Gamma_L + \Gamma_H}{2}, \quad \Delta M = M_H - M_L, \quad \Delta\Gamma = \Gamma_L - \Gamma_H, \tag{1.1}$$

and the CP asymmetry in flavour-specific decays, $a_{\rm fs}$, which quantifies CP violation in mixing. The mass difference $\Delta M = (17.757 \pm 0.021)\,\text{ps}^{-1}$ [1] has been determined very precisely by the CDF [2] and LHCb [3] experiments from the $B_s - \bar{B}_s$ oscillation frequency. The experimental value of the width difference [1],

$$\Delta\Gamma^{\rm exp} = (0.089 \pm 0.006)\,\text{ps}^{-1} \tag{1.2}$$

JHEP10(2017)191

is an average of measurements by LHCb [4, 5], ATLAS [6], CMS [7], and CDF [8]. The average mass $M \equiv M_{B_s}$ and the average width Γ of the mass eigenstates are simply given by the diagonal elements of M and Γ as $M = M_{11} = M_{22}$ and $\Gamma = \Gamma_{11} = \Gamma_{22}$. The remaining physical quantities in $M - i\Gamma/2$ are $|M_{12}|$, $|\Gamma_{12}|$, and the CP-violating phase $\phi_{12} = \arg(-M_{12}/\Gamma_{12})$. These are related to ΔM, $\Delta\Gamma$, and $a_{\rm fs}$ as

$$\Delta M = 2|M_{12}|, \qquad \Delta\Gamma = 2|\Gamma_{12}|\cos\phi_{12} = -\Delta M\,\mathrm{Re}\,\frac{\Gamma_{12}}{M_{12}},$$
$$a_{\rm fs} = \frac{|\Gamma_{12}|}{|M_{12}|}\sin\phi_{12} = \mathrm{Im}\,\frac{\Gamma_{12}}{M_{12}}. \tag{1.3}$$

In these formulas $|\Gamma_{12}| \ll |M_{12}|$ and $|\Delta\Gamma| \ll |\Delta M|$ is used. Within the Standard Model (SM) one finds $\phi_{12} = 0.24^\circ \pm 0.06^\circ$ [9–12], which permits to set $\cos\phi_{12} = 1$ in the SM prediction for $\Delta\Gamma$.

For the calculation of Γ_{12} one employs an operator product expansion, the heavy quark expansion (HQE) [13]–[16], which results in a systematic expansion of Γ_{12} in powers of $\Lambda_{\rm QCD}/m_b \sim 0.1$ and $\alpha_s(m_b) \sim 0.2$. Γ_{12} has been calculated to next-to-leading order (NLO) in both $\Lambda_{\rm QCD}/m_b$ [17] and $\alpha_s(m_b)$ [9, 10, 18, 19]. The leading-power (i.e. $(\Lambda_{\rm QCD}/m_b)^0$) term involves two $|\Delta B| = 2$ operators (B denotes the beauty quantum number)

$$Q = (\bar{s}_i b_i)_{V-A}\,(\bar{s}_j b_j)_{V-A}, \qquad \tilde{Q}_S = (\bar{s}_i b_j)_{S-P}\,(\bar{s}_j b_i)_{S-P}. \tag{1.4}$$

Here the i, j are colour indices and $V \pm A$ means $\gamma_\mu(1 \pm \gamma_5)$ while $S \pm P$ stands for $(1 \pm \gamma_5)$. The hadronic matrix elements, which must be calculated with non-perturbative methods, are usually parameterized as

$$\langle B_s|Q(\mu_2)|\overline{B}_s\rangle = \frac{8}{3}M_{B_s}^2 f_{B_s}^2 B(\mu_2) \qquad \langle B_s|\widetilde{Q}_S(\mu_2)|\overline{B}_s\rangle = \frac{1}{3}M_{B_s}^2 f_{B_s}^2 \widetilde{B}'_S(\mu_2). \tag{1.5}$$

Here f_{B_s} is the B_s decay constant and $\mu_2 = \mathcal{O}(m_b)$ is the renormalization scale at which the matrix elements are calculated. In a lattice-gauge theory calculation μ_2 is the scale at which the lattice-continuum matching is performed. In the expression for Γ_{12} the matrix elements of eq. (1.5) are multiplied by perturbative Wilson coefficients which also depend on μ_2 such that the dependence on the unphysical scale μ_2 cancels from Γ_{12}. In the same way the dependence on the renormalization scheme cancels between the Wilson coefficients and $B(\mu_2)$, $\widetilde{B}'_S(\mu_2)$. In this paper we use the scheme of ref. [18].

$\Delta\Gamma$ is proportional to m_b^2 and the theoretical prediction depends on the renormalization scheme chosen for m_b (for a detailed discussion see ref. [10]) and further on the scale $\mu_1 = \mathcal{O}(m_b)$ at which the $|\Delta B| = 1$ Wilson coefficients are evaluated. Both dependences are unphysical and diminish order-by-order in perturbation theory. At NLO the scheme and scale dependence is still sizable and indicates that higher orders of α_s should be calculated. With up-to-date values for quark masses and the elements of the Cabibbo-Kobayashi-Maskawa (CKM) matrix (stated below in section 5) one finds

$$\Delta\Gamma = (1.74 \pm 0.24)\, f_{B_s}^2 B + (0.40 \pm 0.05) f_{B_s}^2 \widetilde{B}'_S + (-0.65 \pm 0.35)\, f_{B_s}^2 \tag{1.6}$$

JHEP10(2017)191

in the scheme using the pole mass definition of m_b in the prefactor of $\Delta\Gamma$. Here and in the following the hadronic parameters are understood at $\mu_2 = m_b$. The last term in eq. (1.6) is the $\Lambda_{\rm QCD}/m_b$ correction. If instead the $\overline{\rm MS}$ scheme is used for m_b one finds

$$\Delta\Gamma = (1.86 \pm 0.08)\, f_{B_s}^2 B + (0.42 \pm 0.01) f_{B_s}^2 \widetilde{B}'_S + (-0.55 \pm 0.29)\, f_{B_s}^2 \,. \tag{1.7}$$

The errors quoted in the brackets in eqs. (1.6) and (1.7) are found by varying μ_1 between $m_b/2$ and $2m_b$. Ref. [11] has quoted all results for the scheme of eq. (1.7), while in ref. [12] the average of results in the two schemes has been given. A recent lattice calculation [20] has found

$$f_{B_s}^2 B = [0.224\,\text{GeV}]^2\,(1.00 \pm 0.06), \qquad f_{B_s}^2 \widetilde{B}'_S = [0.224\,\text{GeV}]^2\,(1.83 \pm 0.19)\,. \tag{1.8}$$

Here we have added two errors from different sources in quadrature. Ref. [20] has also calculated some of the matrix elements appearing at order $\Lambda_{\rm QCD}/m_b$ and these results went into the last terms of eqs. (1.6) and (1.7). With $f_{B_s} = 0.224\,\text{GeV}$ and neglecting the correlation of the uncertainties in B and $\widetilde{B}'_S$ we find

$$\begin{aligned} \Delta\Gamma &= \left(0.0913 \pm 0.020_{\rm scale} \pm 0.006_{B,\widetilde{B}_S} \pm 0.017_{\Lambda_{\rm QCD}/m_b}\right)\ \text{GeV} \qquad \text{(pole)} \\ \Delta\Gamma &= \left(0.104 \pm 0.008_{\rm scale} \pm 0.007_{B,\widetilde{B}_S} \pm 0.015_{\Lambda_{\rm QCD}/m_b}\right)\ \text{GeV} \qquad (\overline{\rm MS}) \end{aligned} \tag{1.9}$$

From eq. (1.9) we observe that the both scale and scheme dependences exceed the uncertainties from the hadronic parameters B and $\widetilde{B}_S$. Furthermore, the theoretical uncertainty inferred from these dependences is larger than the present experimental error. This calls for a NNLO calculation of the perturbative coefficients multiplying Q and $\widetilde{Q}_S$. In this paper we present the first step in this direction, the calculation of the terms of order $\alpha_s^2 N_f$, where N_f is the number of quark flavours, neglecting quadratic and higher powers of m_c/m_b. Eq. (1.9) will further improve from a future calculation of the NLO corrections to the $\Lambda_{\rm QCD}/m_b$ part and progress in the lattice calculations of the hadronic matrix elements appearing in this order. The contributions of order $(\Lambda_{\rm QCD}/m_b)^2$, however, have been estimated to be small [10, 21]. The theoretical prediction can be further refined, if $\Delta\Gamma$ is predicted from the ratio $\Delta\Gamma/\Delta M$ and the experimental value of ΔM, which is proportional to $f_{B_s}^2 B$. This procedure eliminates the uncertainty associated with B altogether, at the price of making the prediction sensitive to possible new physics in ΔM. From eqs. (1.6) and (1.7) one realises that the numerically dominant term in $\Delta\Gamma/\Delta M$ will not contain any hadronic parameter [10]. This feature also alleviates the problem that the lattice-continuum matching is currently only known to NLO.

This paper is organized as follows: in the following section we summarize the theoretical framework of the calculation. In section 3 we describe details of the renormalization procedure and the regularization of infrared singularities. We present our analytical results in section 4 and perform a phenomenological analysis in section 5. Finally we conclude. Results for matrix elements and master integrals needed for the calculation are relegated to the appendix.

JHEP10(2017)191

2 Theoretical framework

The effective $\Delta B = 1$ weak Hamiltonian, relevant for our calculation, is the following [22]

$$H_{\rm eff}^{\Delta B=1} = \frac{G_F}{\sqrt{2}} V_{cs}^* V_{cb} \left\{ \sum_{i=1}^{6} C_i O_i + C_8 O_8 \right\} \; + \; \text{H.c.}, \tag{2.1}$$

with the operators

$$\begin{aligned}
O_1 &= (\bar{s}_i c_j)_{V-A}\,(\bar{c}_j b_i)_{V-A}, & O_2 &= (\bar{s}_i c_i)_{V-A}\,(\bar{c}_j b_j)_{V-A}, \\
O_3 &= (\bar{s}_i b_i)_{V-A}\,(\bar{q}_j q_j)_{V-A}, & O_4 &= (\bar{s}_i b_j)_{V-A}\,(\bar{q}_j q_i)_{V-A}, \\
O_5 &= (\bar{s}_i b_i)_{V-A}\,(\bar{q}_j q_j)_{V+A}, & O_6 &= (\bar{s}_i b_j)_{V-A}\,(\bar{q}_j q_i)_{V+A}, \\
O_8 &= \frac{g_s}{8\pi^2} m_b \bar{s}_i \sigma^{\mu\nu} (1-\gamma_5) T^a_{ij} b_j G^a_{\mu\nu}.
\end{aligned} \tag{2.2}$$

Here the i, j are colour indices and summation over $q = u, d, s, c, b$ is implied. $V \pm A$ refers to $\gamma_\mu(1 \pm \gamma_5)$ and $S \pm P$ (which we need below) to $(1 \pm \gamma_5)$. $C_1, \ldots, C_6$ and C_8 are the corresponding Wilson coefficient functions. G_F is the Fermi constant and V_{jk} denotes an element of the CKM matrix. Cabbibo-suppressed contributions proportional to $V_{ub}^* V_{us}$ are neglected in (2.1).

To find $\Delta\Gamma \simeq 2|\Gamma_{12}|$ we must calculate

$$\Gamma_{12} = \text{Abs}\langle B_s |\, i \int d^4x \; T\, \mathcal{H}_{\rm eff}(x) \mathcal{H}_{\rm eff}(0) |\bar{B}_s\rangle, \tag{2.3}$$

where 'Abs' denotes the absorptive part of the matrix element and T denotes time ordering. The HQE expresses eq. (2.3) in terms of matrix elements of local operators. The leading term (in powers of $\Lambda_{\rm QCD}/m_b$) reads

$$\Gamma_{12} = \frac{G_F^2 m_b^2}{24\pi\, M_{B_s}} (V_{cb}^* V_{cs})^2 \left[G \,\langle B_s|Q|\bar{B}_s\rangle \; - \; G_S \,\langle B_s|Q_S|\bar{B}_s\rangle \right] \tag{2.4}$$

Using the notation of refs. [9, 10, 18], the coefficients G and G_S are further decomposed as

$$G \;=\; F + P, \qquad G_S \;=\; -F_S - P_S. \tag{2.5}$$

Here F and F_S are the contributions from the current-current operators $Q_{1,2}$ while the small coefficients P and P_S stem from the penguin operators Q_{3-6} and Q_8. The coefficients G, G_S are calculated by expressing the bilocal matrix elements

$$\text{Abs}\,\langle\, i \int d^4x \; T\, Q_i(x) Q_j(0) \,\rangle, \tag{2.6}$$

("full theory") in terms of the local matrix elements $\langle Q\rangle$, $\langle Q_S\rangle$ ("effective theory"), the coefficients of the latter are the desired coefficients. Since G, G_S are short-distance quantities, this matching calculation can be done order-by-order in perturbation theory, with quarks instead of mesons as external states in eq. (2.6). The NLO result of refs. [9, 10, 18, 19] involves eq. (2.6) at the two-loop level for $i, j = 1, 2$. The chromomagnetic operator O_8 is

JHEP10(2017)191

proportional to the strong coupling g_s, so that for $i = 8$ or $j = 8$ a one-loop calculation is sufficient for NLO accuracy. It is further customary to count the small penguin Wilson coefficients C_{3-6} as $\mathcal{O}(\alpha_s)$ and only one-loop diagrams are considered for $i \geq 3$ or $j \geq 3$.

The first ingredient of an NNLO result are the Wilson coefficients of the $\Delta B = 1$ weak Hamiltonian in eq. (2.1). The NNLO Wilson coefficients involve the three-loop anomalous dimension matrix governing the renormalization-group evolution of $C_{1-6,8}$ from the electroweak scale down to the scale $\mu_1 \sim m_b$, at which the matrix elements in eq. (2.6) are evaluated. The NNLO effective hamiltonian has been calculated in refs. [23, 24], albeit in a different operator basis than the one in eq. (2.2), which is used in the NLO calculations of refs. [9, 10, 18, 19] and in this paper.

The NNLO contributions presented in this paper all involve a closed quark loop and would be dominant in the case of a large number N_f of light quarks. However, the limit $N_f \to \infty$ is in conflict with asymptotic freedom of QCD, as the first term β_0 of the QCD β function would change sign. It has been suggested to trade N_f for β_0, so that the $\alpha_s^2 N_f$ term is replaced by a term of order $\alpha_s^2 \beta_0$ (naive non-abelianization [25, 26]). In some applications this procedure gives a good approximation to the full α_s^2 term. However, in quantities involving effective four-quark operators, it is pure speculation whether the original $\alpha_s^2 N_f$ term or its naively non-abelianized version $\propto \alpha_s^2 \beta_0$ approximates the full result in a better way, because neither term cancels the scheme dependence of the operator renormalization. That is, in one scheme the $\alpha_s^2 N_f$ term may be a good approximant, while in another one the $\alpha_s^2 \beta_0$ term does better, or neither of them is sensible. For the standard NDR renormalization scheme used by us, e.g. the calculation in ref. [27] revealed that the $\alpha_s^2 \beta_0$ term is not a good approximation to the full result. In light of this finding we do not advocate the use of naive non-abelianization in our case. Nonetheless, the $\alpha_s^2 N_f$ portion of the full NNLO result is gauge invariant and therefore a meaningful quantity. One can also overcome the scheme-dependence issue by only keeping the $\alpha_s^2 N_f$ terms of the NNLO correction to the RG-improved Wilson coefficients. However, we find that applying this procedure to the known NLO result gives a poor approximation, so that we refrain from using it.

The desired $\alpha_s^2 N_f$ contribution requires the calculation of the diagrams in figure 1. We formally distinguish the charm mass in the lines attached to an effective operator (i.e. to a weak vertex) from that in the charm loop correcting the gluon propagator: the latter give rise to corrections which are linear in m_c/m_b and we keep a non-zero charm mass in these loops. On the contrary, the dependence on the charm mass arising from the lines in which the charm originates from a weak vertex is only quadratic and we use $m_c = 0$ for these lines. Denoting the $\overline{\text{MS}}$-renormalized mass of the quark q with $m_q(\mu)$, where μ is the renormalization scale, we define

$$z = \frac{m_c^2(m_c)}{m_b^2(m_b)} = 0.095, \qquad \text{and} \qquad \bar{z} = \frac{m_c^2(m_b)}{m_b^2(m_b)} = 0.048. \tag{2.7}$$

If the LO and NLO terms are expressed in terms of z, the error associated with the above approximation is of order $\alpha_s^2 N_f z \log^2 z$. If, however, one uses $\bar{z}$ instead, the approximation only inflicts an error of order $\alpha_s^2 N_f \bar{z}$ and the logarithmic terms $\alpha_s^n z \log^n z$, $z = 1, \ldots$ are summed to all orders. This feature has been studied in refs. [10, 28]. The NLO result for $\Delta\Gamma$

JHEP10(2017)191

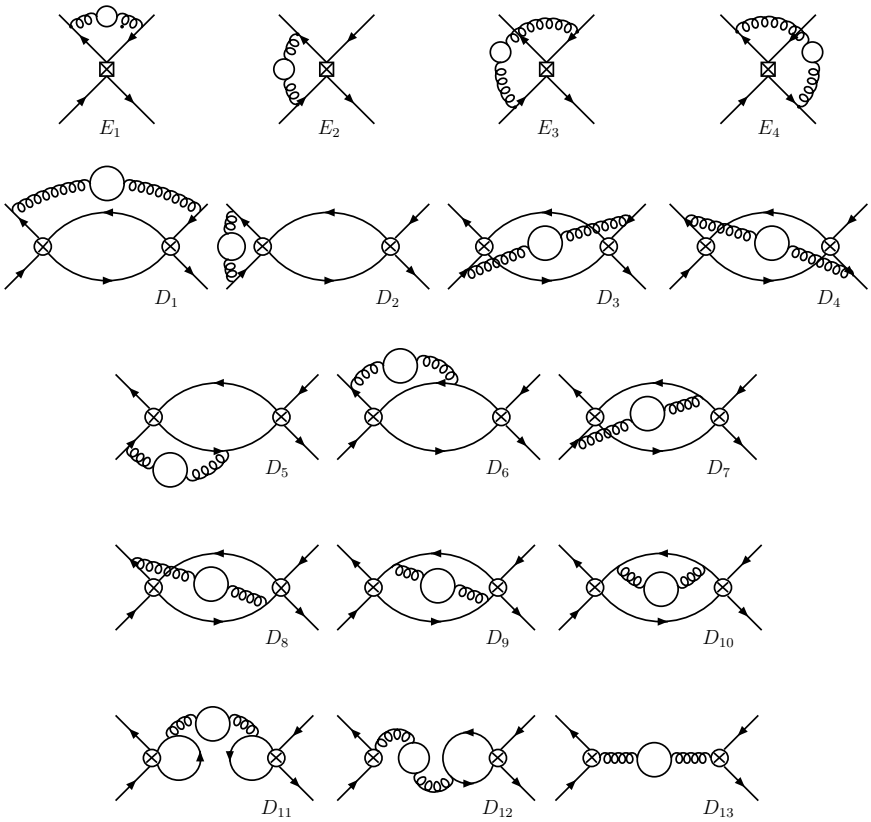

Figure 1. Diagrams $D_1 - D_{13}$ constitute the $O(\alpha_s^2 N_f)$ corrections to eq. (2.6). $E_1 - E_4$ are the corresponding corrections to the matrix elements of local $\Delta B = 2$ operators, which are required for a proper factorization of infrared divergences. Not displayed are E_1', E_2', D_1', D_2', D_5', D_6', D_7', D_8', D_{10}' and D_{12}' which are obtained by rotating the corresponding diagrams by 180^0 and diagrams associated with QCD penguin operators. The closed fermion loop contains massive c, b quarks and massless u, d, s quarks. The charm loop involves terms of order m_c/m_b, so that the charm mass cannot be neglected here. However, in the charm quark lines attached to a weak vertex we set the charm quark mass to zero, which induces an error of order m_c^2/m_b^2.

expressed through $\bar{z}$ is numerically very well reproduced if $\bar{z}$ is set to zero in the NLO correction. Since we discard terms of order $\alpha_s^2 \bar{z}$, one may also expand the z-dependence from the charm quark loop to order $z \log z$ and neglect terms of order z and higher. We calculate the tree-loop diagrams with charm loop indeed as an expansion in z, but keep all terms to order z^3, to check whether the expansion is numerically under good control. Furthermore, a future NNLO calculation keeping higher powers of z terms will benefit from these results.

3 Renormalization and infrared regularization

In this section we specify our renormalization scheme, present the various counterterms, and clarify the regularization procedure used to isolate infrared (IR) divergences. The latter factorize between the full-theory and effective-theory diagrams (see figure 1) and render the desired Wilson coefficients IR-finite.

For the three-loop diagrams involving two insertions of $O_{1,2}$ we need $C_{1,2}$ at NNLO (i.e. calculated with three-loop anomalous dimensions). The result of ref. [23] has been trans-

JHEP10(2017)191

formed to the traditional operator basis in eq. (2.2) in ref. [29] and we use the result of this paper. We renormalize the operators in the usual naive dimensional regularization (NDR) scheme. To fully specify the scheme one must further define the evanescent operators [30]. In ref. [29] the usual NLO definition of these operators has been extended to NNLO in such a way that the diagonal RG evolution of $O_2 \pm O_1$ is maintained at NNLO. For our calculation we must specify the evanescent operators related to Q and $\tilde{Q}_S$: their operational definition involves the following replacements in the D-dimensional Dirac-structures ($D = 4 - 2\epsilon$):

$$[\gamma^\mu\gamma^\nu(1-\gamma_5)]_{ij}[\gamma_\nu\gamma_\mu(1-\gamma_5)]_{kl} \to (8-8\epsilon)[1-\gamma_5]_{il}[1-\gamma_5]_{kj} + 4\epsilon^2[1-\gamma_5]_{ij}[1-\gamma_5]_{kl}, \quad (3.1)$$

$$[\gamma^\mu\gamma^\alpha\gamma^\nu(1-\gamma_5)]_{ij}[\gamma_\nu\gamma_\alpha\gamma_\mu(1-\gamma_5)]_{kl} \to (4-8\epsilon+4\epsilon^2)[\gamma^\mu(1-\gamma_5)]_{ij}[\gamma_\mu(1-\gamma_5)]_{kl}. \quad (3.2)$$

These relations, as well as their colour-flipped counterparts, extend the result of ref. [18] to order ϵ^2. Formally, the evanescent operator $E_1[Q]$ (see ref. [30]) is defined as the difference between the expression on the left and on the right of the arrow in eq. (3.2), supplemented with the quark field operators on the left and right of the Dirac structures, and analogously eq. (3.1) defines $E_1[\tilde{Q}_S]$. At NNLO the ϵ^2 terms matter, and these are chosen to preserve the Fierz symmetry, i.e. the two-loop matrix elements of Q and $\tilde{Q}_S$ are equal to the matrix elements of the operators obtained from Q and $\tilde{Q}_S$ by 4-dimensional Fierz transformations.

In a first step of the calculation the diagrams contributing to eq. (2.6) generate three effective operators, Q, $\tilde{Q}_S$ and $Q_S = (\bar{s}_i b_i)_{S-P}\,(\bar{s}_j b_j)_{S-P}$. However, one linear combination of Q, Q_S, and $\tilde{Q}_S$ is $1/m_b$ suppressed [17], so that one can choose any two of them in the leading-power result addressed in this paper. The $1/m_b$-suppressed operator reads

$$R_0 \equiv Q_S + \alpha_1 \tilde{Q}_S + \alpha_2 \frac{1}{2} Q, \quad (3.3)$$

with $\alpha_{1,2} = 1$ at LO. In ref. [18] it was found that $\alpha_{1,2}$ receive corrections of order α_s. To our order $\alpha_s^2 N_f$ and in the scheme defined by eqs. (3.1) and (3.2) these coefficients read:

$$\begin{aligned}
\alpha_1 = 1 &+ \frac{\alpha_s(\mu_2)}{4\pi} C_f \left(12\log\frac{\mu_2}{m_b} + 6\right) + \frac{\alpha_s^2(\mu_2)}{(4\pi)^2} C_f \left[N_H \left(-\frac{52}{3}\log\frac{\mu_2}{m_b} - 8\log^2\frac{\mu_2}{m_b} - \frac{427}{18} + \frac{8\pi^2}{3}\right)\right. \\
&+ N_V \left(-\frac{52}{3}\log\frac{\mu_2}{m_b} - 8\log^2\frac{\mu_2}{m_b} - \frac{211}{18} - \frac{4\pi^2}{3} + 4\pi^2\sqrt{z} - 24z + 4\pi^2 z^{3/2}\right. \\
&\left. - \frac{1}{9}z^2\left(151 + 12\pi^2 - 78\log z + 18\log^2 z\right) + \frac{8}{75}z^3(19 - 10\log z)\right) \\
&\left. + N_L \left(-\frac{52}{3}\log\frac{\mu_2}{m_b} - 8\log^2\frac{\mu_2}{m_b} - \frac{211}{18} - \frac{4\pi^2}{3}\right)\right], \quad (3.4)
\end{aligned}$$

$$\begin{aligned}
\alpha_2 = 1 &+ \frac{\alpha_s(\mu_2)}{4\pi} C_f \left(6\log\frac{\mu_2}{m_b} + \frac{13}{2}\right) + \frac{\alpha_s^2(\mu_2)}{(4\pi)^2} C_f \left[N_H \left(-\frac{26}{3}\log\frac{\mu_2}{m_b} - 4\log^2\frac{\mu_2}{m_b} - \frac{217}{18} + \frac{4\pi^2}{3}\right)\right. \\
&+ N_V \left(-\frac{26}{3}\log\frac{\mu_2}{m_b} - 4\log^2\frac{\mu_2}{m_b} - \frac{109}{18} - \frac{2\pi^2}{3} + 2\pi^2\sqrt{z} - 12z + 2\pi^2 z^{3/2}\right. \\
&\left. - \frac{1}{18}z^2\left(18\log^2 z - 78\log z + 12\pi^2 + 151\right) + \frac{4}{75}z^3(19 - 10\log z)\right) \\
&\left. + N_L \left(-\frac{26}{3}\log\frac{\mu_2}{m_b} - 4\log^2\frac{\mu_2}{m_b} - \frac{109}{18} - \frac{2\pi^2}{3}\right)\right]. \quad (3.5)
\end{aligned}$$

JHEP10(2017)191

Here $C_f = 4/3$ is a colour factor and μ_2 is the scale at which the operators in eq. (3.3) are defined. $N_H = 1$, $N_V = 1$, and $N_L = 3$ count the numbers of b, c, and light (u, d, s) quarks, respectively. The redundant parameters $N_{H,V}$ are introduced for an easier recognition of the various contributions in the formulae for the coefficients. The results for $\alpha_{1,2}$ are further expanded in z to the third order. Later we will have to express $\alpha_s(\mu_2)$ in terms of $\alpha_s(\mu_1)$, which occurs in the Wilson coefficients. To this end one can use the following formula:

$$\alpha_s(\mu_2) = \alpha_s(\mu_1) + \frac{\alpha_s^2(\mu_1)}{2\pi}\beta_0 \log\frac{\mu_1}{\mu_2}. \tag{3.6}$$

One may freely choose two of the three operators Q, Q_S, and $\tilde{Q}_S$. The choice of the basis $Q, \tilde{Q}_S$ leads to numerically more stable results [10] than the choice Q, Q_S and renders the unknown NLO corrections proportional to $\langle R_0 \rangle$ color-suppressed. Nevertheless the NNLO calculation is more convenient in the latter basis and one may easily transform the result between the bases by using eqs. (3.3) to (3.5).

We next discuss the infrared regularization. For the gluon propagator we use the following expression (similar to the W boson propagator in an R_ξ gauge with $\xi = 0$)

$$\frac{-i\delta_{ab}}{k^2 - m_g^2 + i\epsilon}\left(g_{\mu\nu} - \frac{k_\mu k_\nu}{k^2}\right), \tag{3.7}$$

where m_g is a gluon mass. Our choice of a gluon mass as IR regulator instead of using dimensional regularization has two advantages: in the matching procedure we do not need the ϵ and ϵ^2 parts of NLO and LO Wilson coefficients and the disapperance of m_g from the Wilson coefficients provides a non-trivial check of the calculation.

The NLO renormalization constants of the gluon mass and g_s in $\overline{\text{MS}}$ scheme read [31, 32]

$$\delta Z_x^{(1),N_f} = -\frac{\alpha_s}{2\pi\epsilon}N_f, \qquad \delta Z_{g_s}^{(1),N_f} = \frac{\alpha_s}{6\pi\epsilon}N_f T_R \qquad \text{with } T_R = \frac{1}{2}. \tag{3.8}$$

For the NNLO calculation we need NLO diagrams with counterterms, so that the full-theory NLO diagrams are needed up to order $\mathcal{O}(\epsilon)$. For this reason we have extended the calculation of ref. [18] to order ϵ^1 for $m_c = 0$. Since the two-loop counterterms have $1/\epsilon^2$ poles, we further need the full-theory LO diagrams to order ϵ^2. The results of these diagrams can be found in appendix A.

The NNLO-large-N_f piece of the field renormalization constant for the external quark lines is

$$\delta Z_q^{(2),N_f} = \frac{\alpha_s^2}{(4\pi)^2}\frac{4}{3\epsilon}N_f, \quad q = b, s \tag{3.9}$$

in the 't Hooft-Feynman gauge.

JHEP10(2017)191

We now turn to the counterterms for the $\Delta B = 1$ operators. The hamiltonian in eq. (2.1) reads

$$H_{\rm eff}^{\Delta B=1} = \frac{G_F}{\sqrt{2}} V_{cs}^* V_{cb} \sum_j^6 [C_j O_j]^{\rm bare} = \frac{G_F}{\sqrt{2}} V_{cs}^* V_{cb} \sum_j^6 [C_j O_j]^{\rm ren}$$
$$= \frac{G_F}{\sqrt{2}} V_{cs}^* V_{cb} \sum_{j,k}^6 C_j^{\rm bare} Z_{jk} O_k^{\rm ren} = \frac{G_F}{\sqrt{2}} V_{cs}^* V_{cb} \sum_{j,k}^6 C_j^{\rm ren} Z_{jk} O_k^{\rm bare}. \tag{3.10}$$

The last lines illustrates that one can view Z_{jk} as either renormalising the operator O_k or the Wilson coefficient C_j. Traditionally the renormalization is attributed to the operator, but we adopt the latter viewpoint, with $C_j \equiv C_j^{\rm ren}$ and $O_k \equiv O_k^{\rm bare}$.

Writing $Z_{jk} = \delta_{jk} + \delta Z_{jk}$ and expanding $\delta Z_{jk} = \frac{\alpha_s}{4\pi} \delta Z_{jk}^{(1)} + \left(\frac{\alpha_s}{4\pi}\right)^2 \delta Z_{jk}^{(2)} + \mathcal{O}(\alpha_s^3)$ we find the following counterterms (first calculated in ref. [33]) at order $\alpha_s^2 N_f$:

$$\delta Z_{11}^{(2),N_f} = \delta Z_{22}^{(2),N_f} = -\frac{1}{3} \delta Z_{12}^{(2),N_f} = -\left(\frac{1}{3\epsilon^2} + \frac{1}{18\epsilon}\right) N_f, \tag{3.11}$$

which enters the result for $\Delta\Gamma$ in combination with the LO (one-loop) matrix element $M^{(0)}$ of the full theory given in (A.2).

For the penguin-diagram contributions we need the counterterms δZ_{2k} related to the mixing of O_2 into the four-fermion operators O_{3-6}, necessary to renormalize the penguin diagram D_{11}. There are two types of contributions. The first type induces the mixing between O_2 and O_{3-6}. The non-zero contributions are:

$$\delta Z_{42}^{(1)} = \delta Z_{62}^{(1)} = \frac{1}{3\epsilon}, \tag{3.12}$$

$$\delta Z_{32}^{(2),N_f} = \delta Z_{52}^{(2),N_f} = -\frac{2}{27\epsilon^2} N_f, \tag{3.13}$$

$$\delta Z_{42}^{(2),N_f} = \delta Z_{62}^{(2),N_f} = \frac{2}{9\epsilon^2} N_f. \tag{3.14}$$

In the result for $\Delta\Gamma$ the counterterms in the first line multiply the matrix elements $M_{42}^{(1)}$ and $M_{62}^{(1)}$ in eq. (A.10), while the other (two-loop) counterterms multiply $M_{i2}^{(0)}$, $i = 3, \ldots, 6$, in eq. (A.9). The second type of counterterms involves the mixing of the penguin operators O_{3-6} among themselves. Together with $\delta Z_{42}^{(1)}$ and $\delta Z_{62}^{(1)}$ written above, the additional non-zero contributions, which multiply the $M_{ij}^{(0)}$, $i, j = 3, \ldots, 6$, in eq. (A.15), are:

$$\delta Z_{32}^{(1)} = \delta Z_{52}^{(1)} = -\frac{1}{9\epsilon}. \tag{3.15}$$

Finally we state the $\mathcal{O}(\alpha_s)$ counterterms needed to renormalize the penguin diagram D_{12}. Here the counterterms are $\delta Z_{42}^{(1)}$ and $\delta Z_{62}^{(1)}$ noted above.

In the effective theory the counterterms for gluon mass, strong coupling constant g_s, and external fields (b and s) are treated as in the full theory. For the counterterms of the $\Delta B = 2$ operators note that here only the NNLO renormalization constants can contain parts proportional to N_f, while the NLO renormalization constants have no pieces proportional to N_f. Thus the $\overline{\rm MS}$ renormalization of the $\Delta B = 2$ operators at order $\alpha_s^2 N_f$ is trivial, one just has to drop the divergence from the considered two-loop diagrams with quark loop.

JHEP10(2017)191

4 Results for the coefficients G, G_S at order $\alpha_s^2 N_f$

We first discuss the contributions F,F_S to G,G_S with two insertions of $O_{1,2}$ (see eq. (2.5)). We decompose F defined as

$$F(z) = F_{11}(z)C_1^2(\mu_1) + F_{12}(z)C_1(\mu_1)C_2(\mu_1) + F_{22}(z)C_2^2(\mu_1), \tag{4.1}$$

with an analogous definition of $F_{S,ij}$. We further write

$$F_{ij}(z) = F_{ij}^{(0)}(z) + \frac{\alpha_s(\mu_1)}{4\pi}F_{ij}^{(1)}(z) + \frac{\alpha_s^2(\mu_1)}{(4\pi)^2}\left(N_H F_{ij}^{(2),N_H}(1) + N_V F_{ij}^{(2),N_V}(z) + N_L F_{ij}^{(2),N_L}(0)\right)$$

and similarly for $F_S(z)$. $N_{H,V,L}$ are defined after eq. (3.5). The argument of $F_{ij}^{(2),N_{H,V,L}}$ is the ratio $z_q = m_q^2/m_b^2$, where m_q is the mass of the quark running in the loop in the gluon propagator, i.e. z_q equals 1,z, or 0.

The NNLO functions $F_{ij}^{(2),N_f}$ and $F_{S,ij}^{(2),N_f}$ for the b quark loop read:

$$\begin{aligned}
F_{11}^{(2),N_H}(1) =& -\frac{386}{9}\log\frac{\mu_1}{m_b} + \frac{176}{9}\log\frac{\mu_2}{m_b} - \frac{40}{3}\log\frac{\mu_1}{m_b}\log\frac{\mu_2}{m_b} + \frac{20}{3}\log^2\frac{\mu_2}{m_b} \\
&+\pi^2\left(-\frac{2}{9}\left(1+104\sqrt{5}\right) - \frac{64}{3}\log\frac{1+\sqrt{5}}{2}\right) + \frac{64\zeta(3)}{3} + \frac{95993}{162}, \qquad (4.2)\\
F_{12}^{(2),N_H}(1) =& \frac{554}{27}\log\frac{\mu_1}{m_b} + \frac{352}{27}\log\frac{\mu_2}{m_b} - \frac{80}{9}\log\frac{\mu_1}{m_b}\log\frac{\mu_2}{m_b} + \frac{68}{3}\log^2\frac{\mu_1}{m_b} + \frac{40}{9}\log^2\frac{\mu_2}{m_b} \\
&+\pi^2\left(-\frac{2}{27}\left(53+208\sqrt{5}\right) - \frac{128}{9}\log\frac{1+\sqrt{5}}{2}\right) + \frac{128\zeta(3)}{9} + \frac{518521}{1215}, \qquad (4.3)\\
F_{22}^{(2),N_H}(1) =& \frac{236}{27}\log\frac{\mu_1}{m_b} + \frac{58}{27}\log\frac{\mu_2}{m_b} - \frac{32}{9}\log\frac{\mu_1}{m_b}\log\frac{\mu_2}{m_b} + \frac{20}{3}\log^2\frac{\mu_1}{m_b} + \frac{16}{9}\log^2\frac{\mu_2}{m_b} \\
&+\pi^2\left(\frac{4}{9}\log\frac{\mu_1}{m_b} - \frac{5}{27}\left(12+13\sqrt{5}\right) - \frac{20}{9}\log\frac{1+\sqrt{5}}{2}\right) + \frac{14\zeta(3)}{9} + \frac{99511}{1215}, \qquad (4.4)\\
F_{S,11}^{(2),N_H}(1) =& -\frac{80}{9}\log\frac{\mu_1}{m_b} + \frac{320}{9}\log\frac{\mu_2}{m_b} + \frac{128}{3}\log\frac{\mu_1}{m_b}\log\frac{\mu_2}{m_b} - \frac{64}{3}\log^2\frac{\mu_2}{m_b} \\
&+\pi^2\left(-\frac{16}{9}\left(8+13\sqrt{5}\right) - \frac{64}{3}\log\frac{1+\sqrt{5}}{2}\right) + \frac{64\zeta(3)}{3} + \frac{295238}{405}, \qquad (4.5)\\
F_{S,12}^{(2),N_H}(1) =& \frac{464}{27}\log\frac{\mu_1}{m_b} + \frac{640}{27}\log\frac{\mu_2}{m_b} + \frac{256}{9}\log\frac{\mu_1}{m_b}\log\frac{\mu_2}{m_b} + \frac{32}{3}\log^2\frac{\mu_1}{m_b} - \frac{128}{9}\log^2\frac{\mu_2}{m_b} \\
&+\pi^2\left(-\frac{16}{27}\left(19+26\sqrt{5}\right) - \frac{128}{9}\log\frac{1+\sqrt{5}}{2}\right) + \frac{128\zeta(3)}{9} + \frac{121724}{243}, \qquad (4.6)\\
F_{S,22}^{(2),N_H}(1) =& \frac{704}{27}\log\frac{\mu_1}{m_b} - \frac{320}{27}\log\frac{\mu_2}{m_b} - \frac{128}{9}\log\frac{\mu_1}{m_b}\log\frac{\mu_2}{m_b} + \frac{32}{3}\log^2\frac{\mu_1}{m_b} + \frac{64}{9}\log^2\frac{\mu_2}{m_b} \\
&+\pi^2\left(-\frac{32}{9}\log\frac{\mu_1}{m_b} + \frac{8}{27}\left(30-13\sqrt{5}\right) - \frac{32}{9}\log\frac{1+\sqrt{5}}{2}\right) + \frac{80\zeta(3)}{9} + \frac{5836}{1215}. \qquad (4.7)
\end{aligned}$$

JHEP10(2017)191

The result for the charm loop quark is expanded in $z = m_c^2/m_b^2$ up to $\mathcal{O}(z^3)$:

$$\begin{aligned}
F_{11}^{(2),N_V}(z) = &-42.8889\log\frac{\mu_1}{m_b}+19.5556\log\frac{\mu_2}{m_b}-13.3333\log\frac{\mu_1}{m_b}\log\frac{\mu_2}{m_b}+6.66667\log^2\frac{\mu_2}{m_b}\\
&-5.84736-39.4784\sqrt{z}+z(37-24\log z)-39.4784z^{3/2}\\
&+z^2(2\log^2 z-63.5556\log z+24.5336)\\
&+z^3\left(-14.2222\log^2 z+35.8963\log z+69.8579\right)+\mathcal{O}(z^4), \qquad (4.8)\\
F_{12}^{(2),N_V}(z) = &\,20.5185\log\frac{\mu_1}{m_b}+13.037\log\frac{\mu_2}{m_b}-8.88889\log\frac{\mu_1}{m_b}\log\frac{\mu_2}{m_b}+22.6667\log^2\frac{\mu_1}{m_b}\\
&+4.44444\log^2\frac{\mu_2}{m_b}+40.0184-26.3189\sqrt{z}-z(16\log z+111.333)-26.3189z^{3/2}\\
&+z^2\left(18.3333\log^2 z-117.926\log z+86.7372\right)\\
&+z^3\left(-9.48148\log^2 z+20.9086\log z+62.3882\right)+\mathcal{O}(z^4), \qquad (4.9)\\
F_{22}^{(2),N_V}(z) = &\,13.1272\log\frac{\mu_1}{m_b}+2.14815\log\frac{\mu_2}{m_b}-3.55556\log\frac{\mu_1}{m_b}\log\frac{\mu_2}{m_b}+6.66667\log^2\frac{\mu_1}{m_b}\\
&+1.77778\log^2\frac{\mu_2}{m_b}+20.858-52.6379\sqrt{z}-z(18.1739+32\log z)+35.0919z^{3/2}\\
&+z^2\left(-2.83333\log^2 z-16.6481\log z+13.9138\right)\\
&+z^3\left(-1.48148\log^2 z+9.29383\log z+0.204084\right)+\mathcal{O}(z^4), \qquad (4.10)\\
F_{S,11}^{(2),N_V}(z) = &-8.88889\log\frac{\mu_1}{m_b}+35.5556\log\frac{\mu_2}{m_b}+42.6667\log\frac{\mu_1}{m_b}\log\frac{\mu_2}{m_b}-21.3333\log^2\frac{\mu_2}{m_b}\\
&+82.4693-157.914\sqrt{z}+136z-157.914z^{3/2}\\
&+z^2(8\log^2 z-75.5556\log z+75.1571)\\
&+z^3\left(-14.2222\log^2 z+39.2296\log z+68.3912\right)+\mathcal{O}(z^4), \qquad (4.11)\\
F_{S,12}^{(2),N_V}(z) = &\,17.1852\log\frac{\mu_1}{m_b}+23.7037\log\frac{\mu_2}{m_b}+28.4444\log\frac{\mu_1}{m_b}\log\frac{\mu_2}{m_b}+10.6667\log^2\frac{\mu_1}{m_b}\\
&-14.2222\log^2\frac{\mu_2}{m_b}+75.6462-105.276\sqrt{z}+26.6667z-105.276z^{3/2}\\
&+z^2\left(13.3333\log^2 z-85.9259\log z+83.2254\right)\\
&+z^3\left(-9.48148\log^2 z+24.7309\log z+53.0371\right)+\mathcal{O}(z^4), \qquad (4.12)\\
F_{S,22}^{(2),N_V}(z) = &-9.01785\log\frac{\mu_1}{m_b}-11.8519\log\frac{\mu_2}{m_b}-14.2222\log\frac{\mu_1}{m_b}\log\frac{\mu_2}{m_b}+10.6667\log^2\frac{\mu_1}{m_b}\\
&+7.11111\log^2\frac{\mu_2}{m_b}-42.0084+105.276\sqrt{z}-174.609z+666.747z^{3/2}\\
&+z^2\left(-57.3333\log^2 z+236.296\log z-526.684\right)\\
&+z^3\left(-2.37037\log^2 z+28.5235\log z-32.2992\right)+\mathcal{O}(z^4). \qquad (4.13)
\end{aligned}$$

The contribution of each light quark u, d, s can be obtained by setting $z = 0$ in eqs. (4.8) to (4.13), i.e. $F_{ij}^{(2),N_L}(0) = F_{ij}^{(2),N_V}(0)$.

For the contributions of penguin diagrams and penguin operators in eq. (2.5) we write

$$P(z) = P^{\rm NLO}(z) + \Delta P^{\rm NNLO}(z), \qquad P_S(z) \;=\; P_S^{\rm NLO}(z) + \Delta P_S^{\rm NNLO}(z), \qquad (4.14)$$

where $P^{\rm NLO}(z)$ and $P_S^{\rm NLO}(z)$ are the NLO results of ref. [18], while $\Delta P(z)$ and $\Delta P_S(z)$ are the NNLO corrections with z. Since we treat C_{3-6} as $\mathcal{O}(\alpha_s)$, the latter contain terms of

JHEP10(2017)191

order $C_{3-6}C_{3-6}$, $\alpha_s C_2 C_{3-6}$, and terms of order $\alpha_s^2 C_2^2$. The large-N_f part of $\Delta P^{\rm NNLO}(z)$ is decomposed as

$$\Delta P^{\rm NNLO}(z) = N_H \Delta P^{{\rm NNLO},N_H}(1) + N_V \Delta P^{{\rm NNLO},N_V}(z) + N_L \Delta P^{{\rm NNLO},N_L}(0),$$

with an analogous formula for $\Delta P_S^{\rm NNLO}(z)$. In the penguin contributions the charm mass on all lines touching O_2 are set to zero, while all other charm loops are kept massive. These include not only the loop in D_{11-13}, but also the loops connecting two penguin operators O_{3-6} or one penguin operator and a charm-gluon vertex. The latter two contributions appear in counterterm diagrams (to e.g. D_{11-13}) and must be treated in the same way as the diagrams which they renormalize. Consequently, the argument z_q (with $z_q = 1, z$, or 0) in $\Delta P^{{\rm NNLO},N_{H,V,L}}(z_q)$ refers to the mass in the loop of any of these three situations. (At NNLO there are no diagrams with more than one loop.)

The results are:

$$\Delta P^{{\rm NNLO},N_H}(1) = \frac{\alpha_s(\mu_1)}{4\pi} G_p^{(1),N_H}(1) M_4'(\mu_1) + \frac{\alpha_s^2(\mu_1)}{(4\pi)^2} G_p^{(2),N_H}(1) C_2^2(\mu_1), \tag{4.15}$$

$$\Delta P_S^{{\rm NNLO},N_H}(1) = -\frac{\alpha_s(\mu_1)}{4\pi} 8 G_p^{(1),N_H}(1) M_4'(\mu_1) - \frac{\alpha_s^2(\mu_1)}{(4\pi)^2} 8 G_p^{(2),N_H}(1) C_2^2(\mu_1), \tag{4.16}$$

$$\begin{aligned}\Delta P^{{\rm NNLO},N_V}(z) = {}& \sqrt{1-4z}\left((1-z)M_1'(\mu_1) + \frac{1}{2}(1-4z)M_2'(\mu_1) + 3z M_3'(\mu_1)\right) \\ & + \frac{\alpha_s(\mu_1)}{4\pi} G_p^{(1),N_V}(z) M_4'(\mu_1) + \frac{\alpha_s^2(\mu_1)}{(4\pi)^2} G_p^{(2),N_V}(z) C_2^2(\mu_1),\end{aligned} \tag{4.17}$$

$$\begin{aligned}\Delta P_S^{{\rm NNLO},N_V}(z) = {}& \sqrt{1-4z}\,(1+2z)\left(M_1'(\mu_1) - M_2'(\mu_1)\right) \\ & - \frac{\alpha_s(\mu_1)}{4\pi} 8 G_p^{(1),N_V}(z) M_4'(\mu_1) - \frac{\alpha_s^2(\mu_1)}{(4\pi)^2} 8 G_p^{(2),N_V}(z) C_2^2(\mu_1),\end{aligned} \tag{4.18}$$

with

$$G_p^{(1),N_H}(1) = -\frac{1}{54}\left(6\log\frac{\mu_1}{m_b} - 3\sqrt{3}\pi + 17\right), \tag{4.19}$$

$$G_p^{(2),N_H}(1) = \frac{2}{81}\left(6\log\frac{\mu_1}{m_b} - 3\sqrt{3}\pi + 17\right)\left[2\log\frac{\mu_1}{m_b} + \frac{2}{3} + \frac{3C_8(\mu_1)}{C_2(\mu_1)}\right], \tag{4.20}$$

$$\begin{aligned}G_p^{(1),N_V}(z) = {}& -\frac{1}{54}\left[\sqrt{1-4z}(1+2z)\left(6\log\frac{\mu_1}{m_b} + 3\log\sigma + 2\right) + 6\log\frac{\mu_1}{m_b} - 3\log z + 5 + 12z\right. \\ & \left. + \frac{9C_8(\mu_1)}{C_2(\mu_1)}\sqrt{1-4z}\,(1+2z)\right],\end{aligned} \tag{4.21}$$

$$\begin{aligned}G_p^{(2),N_V}(z) = {}& \frac{1}{81}\left[\frac{4}{3}\left(3\log\frac{\mu_1}{m_b} + 1\right)\left(\sqrt{1-4z}\,(1+2z)\left(3\log\frac{\mu_1}{m_b} + 3\log\sigma + 1\right) + 6\log\frac{\mu_1}{m_b}\right.\right. \\ & \left. - 3\log z + 5 + 12z\right) - 3\pi^2\sqrt{1-4z}\,(1+2z) \\ & + \frac{6C_8(\mu_1)}{C_2(\mu_1)}\left(\sqrt{1-4z}(1+2z)\left(6\log\frac{\mu_1}{m_b} + 3\log\sigma + 2\right) + 6\log\frac{\mu_1}{m_b} - 3\log z + 5 + 12z\right. \\ & \left.\left. + \frac{9C_8(\mu_1)}{2C_2(\mu_1)}\sqrt{1-4z}(1+2z)\right)\right],\end{aligned} \tag{4.22}$$

JHEP10(2017)191

where we have defined $M_1' = 3C_3^2 + 2C_3C_4 + 3C_5^2 + 2C_5C_6$, $M_2' = C_4^2 + C_6^2$, $M_3' = 2(3C_3C_5 + C_3C_6 + C_4C_5 + C_4C_6)$, $M_4' = 2(C_2C_4 + C_2C_6)$ and

$$\sigma = \frac{1 - \sqrt{1-4z}}{1 + \sqrt{1-4z}}. \tag{4.23}$$

As above, $\Delta P^{\mathrm{NNLO},N_L}(0)$ is obtained from eqs. (4.17) and (4.18) by setting z to 0, i.e. $\Delta P^{\mathrm{NNLO},N_L}(0) = \Delta P^{\mathrm{NNLO},N_V}(0)$.

In the matching procedure one has to take into account that the operators, couplings and masses on the full-theory side are defined at the scale μ_1, while the effective operators are defined at the scale μ_2. To compare both sides one must choose the same expansion parameter on both sides, e.g. $\alpha_s(\mu_1)$, and use eq. (3.6) for this. Therefore the $\alpha_s^2 N_f$ results quoted in this section also contain contributions from the α_s^1 parts through eq. (3.6).

5 Phenomenology of $\Delta\Gamma$

In this section we show the impact of the new $\alpha_s^2 N_f$ terms on $\Delta\Gamma_s$. Our input parameters are collected in table 1. We use the complete NNLO $\Delta B = 1$ Wilson coefficients C_1, C_2 [29] and the complete NLO expressions for $C_3, \dots C_6$, with the numerical values listed in table 2. The $\alpha_s^2 N_f^0$ terms of the coefficients inflict a scheme dependence on $\Delta\Gamma$, which will only be cancelled once the full NNLO calculation is performed. Nevertheless we can study whether the new large-N_f terms help to reduce scale and scheme dependences.

The coefficients $G = F + P$ and $G_S = -F_S - P_S$ correspond to the pole scheme for $\Delta\Gamma$. For the $\overline{\mathrm{MS}}$ scheme we must multiply these coefficients with $\bar{m}_b^2/m_b^{\mathrm{pole}}$ and expand this ratio to the order in α_s to which G, G_s are calculated [10], in our case this is $\mathcal{O}(\alpha_s^2 N_f)$. In both schemes we use $\bar{z}$ defined in eq. (2.7); the transformation from z to $\bar{z}$ in the NLO formula can be found in eq. (18) of ref. [28]. Since we have set $z = 0$ in the charm lines attached to weak vertices, no NNLO corrections to the transformation occur.

We further must calculate m_b^{pole} from $\bar{m}_b$ and we use the full 2-loop result for this [34–36]. This is a reasonable approach, if the missing $\alpha_s^2 N_f^0$ in the $\overline{\mathrm{MS}}$ scheme have the expected $\mathcal{O}(10\%)$ size while being larger in the pole scheme to compensate for the anomalously large ratio $m_b^{\mathrm{pole}\,2}/\bar{m}_b^2 \sim 1.3$.

In both $\overline{\mathrm{MS}}$ and pole scheme we use $\bar{m}_b(\bar{m}_b) = (4.18 \pm 0.03)\,\mathrm{GeV}$ as input and calculate $m_b^{\mathrm{pole}} = 4.58\mathrm{GeV}$ at NLO and $m_b^{\mathrm{pole}} = 4.85\mathrm{GeV}$ at order α_s^2. In eq. (1.9) we find a small scale dependence in the $\overline{\mathrm{MS}}$ scheme, because the sizable μ_1 dependence of the prefactor $\bar{m}_b(\mu_1)^2$ cancels nicely with the μ_1 dependence of G,G_S. In our partial NNLO result this efficient cancellation is less pronounced than in the NLO result of eq. (1.9). To be conservative, we therefore use a different approach in this section: we keep $\bar{m}_b(\bar{m}_b)^2$ fixed and, for consistency, also eliminate the $\log(\mu_1/\bar{m}_b)$ terms related to the running of $\bar{m}_b$ from G,G_S. This leads to a larger μ_1 dependence at NLO.

JHEP10(2017)191

$\bar{m}_b(\bar{m}_b) =$	$(4.18 \pm 0.03)\,\text{GeV}$	[37]	$\bar{m}_c(\bar{m}_c) =$	$(1.286 \pm 0.013_{\text{stat}} \pm 0.040_{\text{syst}})\,\text{GeV}$	[38–40][a]
$\bar{m}_s(\bar{m}_b) =$	$(0.079 \pm 0.002)\,\text{GeV}$	[20, 41]	$\bar{m}_t(m_t) =$	$(165.96 \pm 0.35_{\text{stat}} \pm 0.64_{\text{syst}})\,\text{GeV}$	[38][a]
$\lvert V_{cb}\rvert =$	$41.80^{+0.33}_{-0.68} \cdot 10^{-3}$	[38][a]	$\lvert V_{ub}\rvert =$	$3.714^{+0.07}_{-0.06} \cdot 10^{-3}$	[38][a]
$\gamma =$	$68^\circ{}^{+0.9^\circ}_{-2.0^\circ}$	[38][a]	$m_b^{\text{pow}} =$	$4.7\,\text{GeV}$	see [10]
$f_{B_s}\sqrt{\widetilde{B}'_S} =$	$303\,\text{MeV}$	[20]	$\widetilde{B}_{R_0} =$	0.56 ± 0.53	[20]
$f_{B_s}\sqrt{B} =$	$224\,\text{MeV}$	[20]			
$M_{B_s} =$	$5.368\,\text{GeV}$	[37]	$\alpha_s(M_Z) =$	0.1185	
$\lvert V_{ts}^* V_{tb}\rvert =$	$40.9 \cdot 10^{-3}$				

[a]We use updated numbers from http://ckmfitter.in2p3.fr.

Table 1. Input parameters used in section 5. $\bar{m}_s(\bar{m}_b)$ is calculated from $\bar{m}_s(2\text{GeV}) = 0.094 \pm 0.001\,\text{GeV}$ [41]. m_B^{pow} is a redundant parameter calibrating the overall size of the hadronic parameters B_{R_i} which quantify the matrix elements at order Λ_{QCD}/m_b. The translation of $\langle R_0\rangle = -0.19 \pm 0.18\,\text{GeV}$ [20] to $\widetilde{B}_{R_0}$ for our choice of m_b^{pow} is done with $f_{B_s} = (0.224 \pm 0.05)\,\text{GeV}$ [41]. Subsequently this result is used to rescale $\widetilde{B}_{R_0}/B$ from the value in ref. [20] to the one in the table. $\widetilde{B}_S$ is larger than $\widetilde{B}'_S$ by a factor of $M_{B_s}^2/(\bar{m}_b + \bar{m}_s)^2 = 1.588$, so that $\widetilde{B}'_S/B = 1.83 \pm 0.21$.

i	$C_i^{(0)}(\mu_b)$	$C_i^{(1)}(\mu_b)$	$C_i^{(2)}(\mu_b)$
1	-0.2687	4.332	50.142
2	1.1179	-2.024	-17.114
3	0.0121	0.090	–
4	-0.0274	-0.465	–
5	0.0079	0.041	–
6	-0.0343	-0.434	–
8	-0.1508	-1.0006	–

Table 2. The LO, NLO and NNLO Wilson coefficients $C_i^{(k)}(\mu_b)$ at $\mu_b = \bar{m}_b = 4.18$ GeV using $\alpha_s(\bar{m}_b) = 0.226$ (implementing the formula of ref. [42] with QED effects set to zero) and the matching scale $\mu_0 = M_W$. We have used ref. [29] to compute $C_1^{(k)}(\mu_b)$ and $C_2^{(k)}(\mu_b)$. The NLO piece of the Wilson coefficient $C_8^{(1)}$ is taken from the calculation in a different basis [24] and the quoted value therefore neglects a numerically small contribution from an evanescent operator.

We find:

$$\begin{aligned}
\Delta\Gamma^{\text{NLO}} &= (0.091 \pm 0.020_{\text{scale}})\ \text{GeV} \qquad (\text{pole}) \\
\Delta\Gamma^{\text{NLO}} &= (0.104 \pm 0.015_{\text{scale}})\ \text{GeV} \qquad (\overline{\text{MS}}) \qquad (5.1) \\
\Delta\Gamma^{\text{NNLO}} &= (0.108 \pm 0.021_{\text{scale}})\ \text{GeV} \qquad (\text{pole}) \\
\Delta\Gamma^{\text{NNLO}} &= (0.103 \pm 0.015_{\text{scale}})\ \text{GeV} \qquad (\overline{\text{MS}}) \qquad (5.2)
\end{aligned}$$

where the scale dependence is calculated by varying μ_1 between $m_b/2$ and $2m_b$ and for the quoted central values of $\Delta\Gamma$ we took $\mu_1 = m_b^{\text{pole}}$ and $\mu_1 = \bar{m}_b$ for the pole and $\overline{\text{MS}}$

JHEP10(2017)191

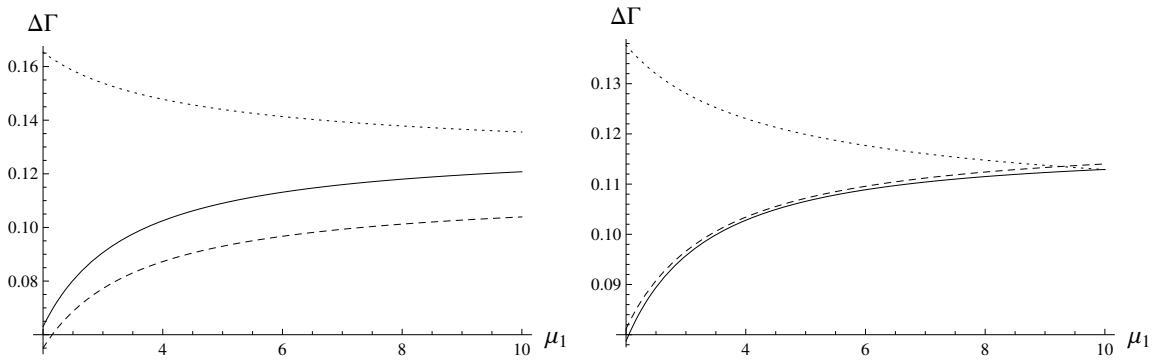

Figure 2. Renormalization scale dependence for $\Delta\Gamma$ at LO (dotted), NLO (dashed), and NNLO (solid) results for the pole scheme (left) and the $\overline{\text{MS}}$ scheme (right). On the x axis is μ_1 in GeV-s.

schemes, respectively. Unlike in eq. (1.9) other sources of error are neglected here. The μ_1 dependence is plotted in figure 2.

We observe that the partial NNLO corrections calculated in this section decrease the scheme dependence and give preference to the NLO result in the $\overline{\text{MS}}$ scheme. The result also suggests that in eq. (1.9) the μ_1 dependence is underestimated and that the partial NNLO calculation does not reduce the scale dependence to a satisfactory level.

We have discussed the naive non-abelianization approach (NNA) in section 2. If we trade N_f for β_0 in G, G_S and the relation between $\bar{m}_b = 4.18\,\text{GeV}$ and m_b^{pole}, we find $m_b^{\text{pole}} = 4.87\,\text{GeV}$, which is close to the full two-loop result, and

$$\begin{aligned}\Delta\Gamma^{\text{NNA}} &= (0.071 \pm 0.020_{\text{scale}})\ \text{GeV} \qquad (\text{pole})\\ \Delta\Gamma^{\text{NNA}} &= (0.099 \pm 0.012_{\text{scale}})\ \text{GeV} \qquad (\overline{\text{MS}}).\end{aligned} \tag{5.3}$$

Comparing eq. (5.2) with eq. (5.3) we find that the $\overline{\text{MS}}$ result is quite stable, if we change the literal $\alpha_s^2 N_f$ result to the NNA one, while the pole-scheme result is not.

Until a full NNLO calculation is available, we recommend to use the $\overline{\text{MS}}$ NLO value with an enlarged μ_1 dependence compared to eqs. (1.7) and (1.9):

$$\begin{aligned}\Delta\Gamma &= (1.86 \pm 0.17)\, f_{B_s}^2 B + (0.42 \pm 0.03) f_{B_s}^2 \widetilde{B}'_S + (-0.55 \pm 0.29)\, f_{B_s}^2 .\\ \Delta\Gamma &= \left(0.104 \pm 0.015_{\text{scale}} \pm 0.007_{B,\widetilde{B}_S} \pm 0.015_{\Lambda_{\text{QCD}}/m_b}\right)\ \text{GeV} \qquad (\overline{\text{MS}})\end{aligned} \tag{5.4}$$

6 Conclusions

We have calculated the contributions of order $\alpha_s^2 N_f$ to the width difference in the $B_s - \bar{B}_s$ system in an expansion in m_c/m_b, neglecting terms of order $(m_c/m_b)^2$ and higher. This calculation has involved three-loop massive master integrals with two mass scales. We find a larger correction for the decay width difference in the pole scheme and only a minuscule correction for the $\overline{\text{MS}}$ scheme. As a result, the scheme dependence reduces considerably and we advocate the use of the NLO numerical values in eq. (5.4).

JHEP10(2017)191

Acknowledgments

We would like to thank Christoph Greub for helpful discussions. This work has been supported by Grant No. 86426 of the Volkswagen Stiftung. H.A., A.H. and A.Y. were further supported by the State Committee of Science of Armenia Program Grant No. 15T-1C161 and U.N. has received support from BMBF under contract no. 05H15VKKB1.

A Full-theory matrix elements

In this section we collect the needed unrenormalized LO and NLO matrix elements to order ϵ^2 and ϵ, respectively. We decompose the matrix element as

$$M = M_{\rm cc} + M_{\rm peng}, \tag{A.1}$$

where the first term denotes the contribution with two insertions of the current-current operators $O_{1,2}$ and the second term comprises the diagrams with at least one penguin operator. Recall that we count C_{3-6} as order α_s, so that one loop less is needed for $M_{\rm peng}$ compared to $M_{\rm cc}$. We expand $M_{\rm cc,peng} = M^{(0)}_{\rm cc,peng} + \frac{\alpha_s}{4\pi} M^{(1)}_{\rm cc,peng} + \ldots$ and quote all results for $m_c = 0$.

A.1 Current-current operators

The LO full-theory result $M^{(0)}_{\rm cc}$ is needed to order $\mathcal{O}(\epsilon^2)$:

$$\begin{aligned} M^{(0)}_{\rm cc} = &-\frac{G_F^2 m_b^2}{12\pi}(V_{cs}^* V_{cb})^2 \left(\left(3C_1^{b2}+2C_1^b C_2^b\right)\left(\frac{1}{2}\langle Q\rangle^{(0)} - \langle \tilde{Q}_S\rangle^{(0)}\right) + C_2^{b2}\left(\langle Q\rangle^{(0)} + \langle \tilde{Q}_S\rangle^{(0)}\right)\right) \\ &\cdot\left(1+\epsilon\left(\frac{2}{3}+2\log\frac{\mu_1}{m_b}\right)+\epsilon^2\left(2\log^2\frac{\mu_1}{m_b}+\frac{4}{3}\log\frac{\mu_1}{m_b}-\frac{\pi^2}{4}+\frac{13}{9}\right)\right), \end{aligned} \tag{A.2}$$

Here and in the following $\langle\ldots\rangle^{(0)}$ denote tree-level matrix elements and $C_k^b = \sum_j C_j Z_{jk}$ are bare Wilson coefficients (see eq. (3.10)).

We decompose the NLO diagrams according to the diagrams in figure 1 and the Wilson coefficients as

$$M^{(1)}_{\rm cc} = -\frac{G_F^2 m_b^2}{12\pi}(V_{cs}^* V_{cb})^2 \left(M^{(1)}_{11,D_{1-10}} + M^{(1)}_{12,D_{1-10}} + M^{(1)}_{22,D_{1-10}} + M^{(1)}_{D_{11}} + M^{(1)}_{D_{12}}\right) \tag{A.3}$$

The sum of the full-theory non-penguin NLO diagrams amounts to

$$\begin{aligned} M^{(1)}_{11,D_{1-10}} = C_1^{b2}\Bigg(&\langle Q\rangle^{(0)}\left[-\frac{17}{3}-4\log\frac{\mu_1}{m_b}+4\log\frac{\mu_1}{m_g}+\epsilon\left(\log\frac{\mu_1}{m_b}\left(8\log\frac{\mu_1}{m_g}-\frac{125}{6}\right)\right.\right. \\ &\left.\left. - 12\log^2\frac{\mu_1}{m_b}+4\log^2\frac{\mu_1}{m_g}-\frac{11}{6}\log\frac{\mu_1}{m_g}-48\zeta(3)+\frac{4\pi^2}{3}+\frac{565}{72}\right)\right] \\ &+\langle \tilde{Q}_S\rangle^{(0)}\left[\frac{4}{3}-16\log\frac{\mu_1}{m_b}+16\log\frac{\mu_1}{m_g}+\epsilon\left(\log\frac{\mu_1}{m_b}\left(32\log\frac{\mu_1}{m_g}-\frac{28}{3}\right)\right.\right. \\ &\left.\left. - 48\log^2\frac{\mu_1}{m_b}+16\log^2\frac{\mu_1}{m_g}+\frac{44}{3}\log\frac{\mu_1}{m_g}+96\zeta(3)+\frac{16\pi^2}{3}-\frac{671}{9}\right)\right]\Bigg), \end{aligned} \tag{A.4}$$

JHEP10(2017)191

$$
\begin{aligned}
&M^{(1)}_{12,D_{1-10}}\\
&=2C_1^bC_2^b\bigg(\langle Q\rangle^{(0)}\bigg[-\frac{13}{2\epsilon}-\frac{385}{18}-\frac{82}{3}\log\frac{\mu_1}{m_b}+\frac{4}{3}\log\frac{\mu_1}{m_g}+\epsilon\bigg(\log\frac{\mu_1}{m_b}\bigg(\frac{8}{3}\log\frac{\mu_1}{m_g}-\frac{1529}{18}\bigg)\\
&\qquad-56\log^2\frac{\mu_1}{m_b}+\frac{4}{3}\log^2\frac{\mu_1}{m_g}-\frac{11}{18}\log\frac{\mu_1}{m_g}-16\zeta(3)+\frac{133\pi^2}{36}-\frac{9263}{216}\bigg)\bigg]\\
&\quad+\langle\tilde{Q}_S\rangle^{(0)}\bigg[\frac{4}{\epsilon}+\frac{112}{9}+\frac{32}{3}\log\frac{\mu_1}{m_b}+\frac{16}{3}\log\frac{\mu_1}{m_g}+\epsilon\bigg(\log\frac{\mu_1}{m_b}\bigg(\frac{32}{3}\log\frac{\mu_1}{m_g}+\frac{404}{9}\bigg)\\
&\qquad+16\log^2\frac{\mu_1}{m_b}+\frac{16}{3}\log^2\frac{\mu_1}{m_g}+\frac{44}{9}\log\frac{\mu_1}{m_g}+32\zeta(3)-\frac{2\pi^2}{9}+\frac{85}{27}\bigg)\bigg]\bigg),
\end{aligned}
\tag{A.5}
$$

$$
\begin{aligned}
&M^{(1)}_{22,D_{1-10}}\\
&=C_2^{b2}\bigg(\langle Q\rangle^{(0)}\bigg[-\frac{1}{\epsilon}-\frac{11}{18}-\frac{5}{3}\pi^2-\frac{8}{3}\log\frac{\mu_1}{m_b}-\frac{4}{3}\log\frac{\mu_1}{m_g}+\epsilon\bigg(\log\frac{\mu_1}{m_b}\bigg(\frac{11}{18}-\frac{20\pi^2}{3}-\frac{8}{3}\log\frac{\mu_1}{m_g}\bigg)\\
&\qquad-4\log^2\frac{\mu_1}{m_b}-\frac{4}{3}\log^2\frac{\mu_1}{m_g}-\frac{55}{18}\log\frac{\mu_1}{m_g}-22\zeta(3)-\frac{49\pi^2}{18}+\frac{445}{24}\bigg)\bigg]\\
&\quad+\langle\tilde{Q}_S\rangle^{(0)}\bigg[\frac{8}{\epsilon}-\frac{8}{3}\pi^2+\frac{320}{9}+\frac{112}{3}\log\frac{\mu_1}{m_b}-\frac{16}{3}\log\frac{\mu_1}{m_g}+\epsilon\bigg(\log\frac{\mu_1}{m_b}\bigg(\frac{1324}{9}-\frac{32}{3}\pi^2-\frac{32}{3}\log\frac{\mu_1}{m_g}\bigg)\\
&\qquad+80\log^2\frac{\mu_1}{m_b}-\frac{16}{3}\log^2\frac{\mu_1}{m_g}-\frac{44}{9}\log\frac{\mu_1}{m_g}-16\zeta(3)-\frac{92\pi^2}{9}+\frac{3443}{27}\bigg)\bigg]\bigg).
\end{aligned}
\tag{A.6}
$$

and for the penguin diagrams

$$
\begin{aligned}
M^{(1)}_{D_{11}}&=-\frac{5\langle Q\rangle^{(0)}+8\langle\tilde{Q}_S\rangle^{(0)}}{9}C_{b2}^2\bigg(\frac{1}{\epsilon}+\frac{4}{3}+4\log\frac{\mu_1}{m_b}+\epsilon\bigg(\frac{10}{3}-\frac{5}{6}\pi^2+\frac{16}{3}\log\frac{\mu_1}{m_b}+8\log^2\frac{\mu_1}{m_b}\bigg)\bigg),\\
M^{(1)}_{D_{12}}&=-\frac{1}{3}(5\langle Q\rangle^{(0)}+8\langle\tilde{Q}_S\rangle^{(0)})C_2^bC_8^b\bigg(1+\epsilon\bigg(\frac{2}{3}+2\log\frac{\mu_1}{m_b}\bigg)\bigg).
\end{aligned}
\tag{A.7}
$$

A.2 Penguin operators

For the matrix elements with two QCD penguin operators we write

$$
M_{\rm peng}=-\frac{G_F^2m_b^2}{12\pi}(V_{cs}^*V_{cb})^2\left[\sum_{j=3}^{6}M_{j2}+\sum_{\substack{j=3\\j\le k}}^{6}M_{jk}\right]
\tag{A.8}
$$

As usual we expand M_{jk} as $M_{jk}=M_{jk}^{(0)}+\frac{\alpha_s}{4\pi}M_{jk}^{(1)}+\ldots$. The unrenormalized LO and NLO matrix elements necessary for the renormalization of the penguin diagrams D_{11} and D_{12} are the following:

$$
\begin{aligned}
M_{32}^{(0)}&=2C_2^bC_3^bF_3, & M_{42}^{(0)}&=2C_2^bC_4^bF_4,\\
M_{52}^{(0)}&=0, & M_{62}^{(0)}&=0,
\end{aligned}
\tag{A.9}
$$

$$
\begin{aligned}
M_{42}^{(1)}&=2C_2^bC_4^b(F_1+F_2), & M_{62}^{(1)}&=2C_2^bC_6^b(F_1+F_2)
\end{aligned}
\tag{A.10}
$$

JHEP10(2017)191

where

$$F_1 = -\frac{1}{9}(8\langle\tilde{Q}_S\rangle^{(0)}+5\langle Q\rangle^{(0)})\left[\frac{1}{2\epsilon}+2\log\frac{\mu_1}{m_b}+\frac{1}{6}\left(19-3\sqrt{3}\pi\right)\right. \tag{A.11}$$
$$+\epsilon\left(\frac{1}{4}\sqrt{3}\pi\log 3-\frac{\pi^2}{12}+\left(\frac{19}{3}-\sqrt{3}\pi\right)\left(2\log\frac{\mu_1}{m_b}+\frac{3}{2}\right)+4\log^2\frac{\mu_1}{m_b}\right.$$
$$\left.\left.-\frac{3}{2}i\sqrt{3}\left(\mathrm{Li}_2\left(\frac{1}{2}-\frac{i}{2\sqrt{3}}\right)-\mathrm{Li}_2\left(\frac{1}{2}+\frac{i}{2\sqrt{3}}\right)\right)\right)\right],$$

$$F_2 = -\frac{1}{9}(8\langle\tilde{Q}_S\rangle^{(0)}+5\langle Q\rangle^{(0)})\left[\frac{\frac{1}{2}+\sqrt{1-4z}\left(\frac{1}{2}+z\right)}{\epsilon}+2\log\frac{\mu_1}{m_b}+\frac{7}{6}+2z-\frac{1}{2}\log(1-4z)\right. \tag{A.12}$$
$$+\log(1-\sigma)-\frac{\log\sigma}{2}+\frac{1}{6}\sqrt{1-4z}\left(7+20z+3(2z+1)\left(4\log\frac{\mu_1}{m_b}+\log\sigma-\log(1-4z)\right)\right)$$
$$+\epsilon\frac{1}{12}\left(34-\pi^2+80z-2\log(1-4z)\left(12\log\frac{\mu_1}{m_b}+7+12z+6\log(1-\sigma)-3\log\sigma\right)\right.$$
$$+8\left(7+12z+6\log(1-\sigma)-3\log\sigma\right)\log\frac{\mu_1}{m_b}+48\log^2\frac{\mu_1}{m_b}+3\log^2(1-4z)$$
$$+(2\log(1-\sigma)-\log\sigma)(24z+6\log(1-\sigma)-3\log\sigma+14)$$
$$+\sqrt{1-4z}\left(34+108z+2(20z+7)\left(4\log\frac{\mu_1}{m_b}-\log(1-4z)+\log\sigma\right)\right.$$
$$\left.\left.\left.+\ 3(2z+1)\left(\left(4\log\frac{\mu_1}{m_b}-\log(1-4z)+\log\sigma\right)^2-4\mathrm{Li}_2(\sigma)-2\log^2\sigma-3\pi^2\right)\right)\right)\right],$$

and

$$F_3 = \left(\frac{1}{2}\langle Q\rangle^{(0)}-\langle\tilde{Q}_S\rangle^{(0)}\right)\left[1+\epsilon\left(\frac{2}{3}+2\log\frac{\mu_1}{m_b}\right)+\epsilon^2\left(2\log^2\frac{\mu_1}{m_b}+\frac{4}{3}\log\frac{\mu_1}{m_b}-\frac{\pi^2}{4}+\frac{13}{9}\right)\right], \tag{A.13}$$

$$F_4 = \left(\langle Q\rangle^{(0)}+\langle\tilde{Q}_S\rangle^{(0)}\right)\left[1+\epsilon\left(\frac{2}{3}+2\log\frac{\mu_1}{m_b}\right)+\epsilon^2\left(2\log^2\frac{\mu_1}{m_b}+\frac{4}{3}\log\frac{\mu_1}{m_b}-\frac{\pi^2}{4}+\frac{13}{9}\right)\right]. \tag{A.14}$$

We only need the LO contributions $M_{jk}^{(0)}$ for $j,k\geq 3$:

$$\begin{aligned}
M_{33}^{(0)} &= 3C_3^{b2}\hat{F}_5, & M_{34}^{(0)} &= 2C_3^bC_4^b\hat{F}_5,\\
M_{35}^{(0)} &= 6C_3^bC_5^b\hat{F}_7, & M_{36}^{(0)} &= 2C_3^bC_6^b\hat{F}_7,\\
M_{44}^{(0)} &= C_4^{b2}\hat{F}_6, & M_{45}^{(0)} &= 2C_4^bC_5^b\hat{F}_7,\\
M_{46}^{(0)} &= 2C_4^bC_6^b\hat{F}_7, & M_{55}^{(0)} &= 3C_5^{b2}\hat{F}_5,\\
M_{56}^{(0)} &= 2C_5^bC_6^b\hat{F}_5, & M_{66}^{(0)} &= C_6^{b2}\hat{F}_6,
\end{aligned} \tag{A.15}$$

JHEP10(2017)191

We need the coefficient functions up to ϵ^2, finding

$$\begin{aligned}
\hat{F}_5 = \sqrt{1-4z}\Bigg[&\frac{1}{2}\langle Q\rangle^{(0)}(1-4z) - \langle \tilde{Q}_S\rangle^{(0)}(2z+1) \\
&+\frac{1}{3}\epsilon\left(\frac{1}{2}\langle Q\rangle^{(0)}(1-4z)\left(5+6\log\frac{\mu_1}{m_b}-3\log(1-4z)\right)\right. \\
&\left.-\langle \tilde{Q}_S\rangle^{(0)}\left(5+16z-3(2z+1)\left(2\log\frac{\mu_1}{m_b}-\log(1-4z)\right)\right)\right) \\
&+\frac{1}{36}\epsilon^2\left(\frac{1}{2}\langle Q\rangle^{(0)}(1-4z)\left(112-9\pi^2+60\left(2\log\frac{\mu_1}{m_b}-\log(1-4z)\right)\right.\right. \\
&\left.+18\left(2\log\frac{\mu_1}{m_b}-\log(1-4z)\right)^2\right) \\
&-\langle \tilde{Q}_S\rangle^{(0)}\left(112+416z-9\pi^2(2z+1)+12(16z+5)\left(2\log\frac{\mu_1}{m_b}-\log(1-4z)\right)\right. \\
&\left.\left.\left.+18(2z+1)\left(2\log\frac{\mu_1}{m_b}-\log(1-4z)\right)^2\right)\right)\Bigg], \qquad \text{(A.16)}
\end{aligned}$$

$$\begin{aligned}
\hat{F}_6 = \sqrt{1-4z}\Bigg[&\langle Q\rangle^{(0)}(1-z) + \langle \tilde{Q}_S\rangle^{(0)}(2z+1) \\
&+\frac{1}{3}\epsilon\left(\langle Q\rangle^{(0)}\left(5-2z+3(1-z)(2\log\frac{\mu_1}{m_b}-\log(1-4z))\right)\right. \\
&\left.+\langle \tilde{Q}_S\rangle^{(0)}\left(5+16z+3(2z+1)\left(2\log\frac{\mu_1}{m_b}-\log(1-4z)\right)\right)\right) \\
&+\frac{1}{36}\epsilon^2\left(\langle Q\rangle^{(0)}\left(112-16z-9\pi^2(1-z)+12(5-2z)\left(2\log\frac{\mu_1}{m_b}-\log(1-4z)\right)\right.\right. \\
&\left.+18(1-z)\left(2\log\frac{\mu_1}{m_b}-\log(1-4z)\right)^2\right) \\
&+\langle \tilde{Q}_S\rangle^{(0)}\left(112+416z-9\pi^2(2z+1)+12(16z+5)\left(2\log\frac{\mu_1}{m_b}-\log(1-4z)\right)\right. \\
&\left.\left.\left.+18(2z+1)\left(2\log\frac{\mu_1}{m_b}-\log(1-4z)\right)^2\right)\right)\Bigg], \qquad \text{(A.17)}
\end{aligned}$$

$$\begin{aligned}
\hat{F}_7 = \langle Q\rangle^{(0)} z\sqrt{1-4z}&\left(3+3\epsilon\left(2+2\log\frac{\mu_1}{m_b}-\log(1-4z)\right)\right. \\
&\left.+\frac{3}{4}\epsilon^2\left(\pi^2-16+2\left(4+2\log\frac{\mu_1}{m_b}-\log(1-4z)\right)\left(2\log\frac{\mu_1}{m_b}-\log(1-4z)\right)\right)\right). \qquad \text{(A.18)}
\end{aligned}$$

The $M_{25}^{(0)}$ and $M_{26}^{(0)}$ (due to the $(V-A)\otimes(V+A)$ chiral structure) are proportional to m_c^2 and vanish in our approximation $m_c = 0$ for the charm lines attached to weak vertices.

JHEP10(2017)191

B Results of master integrals

We have reduced the Feynman diagrams shown on figure 1 to master integrals by means of the program FIRE [43]. For the full-theory diagrams we have calculated the absorptive part of master integrals, i.e. the 2-, 3-, 4- particle cuts with a massive c-, b-quarks in the closed fermion loop, with a massive gluon in infrared singular diagrams and a massless c-quark in the weak loop, using formulas for phase space integrals derived in [44]. For some integrals, with massive charm, we used a Mellin-Barnes representation [45] and expanded in terms of the small parameter $z = m_c^2/m_b^2$. The master integrals, which include m_g, are expanded over $z_g = m_g^2/m_b^2$. The results of master integrals have been checked numerically by means of the program SecDec-3 [46].

The results for diagrams with massless u-, d-, s-quarks in the closed fermion loop are obtained by taking the limit $m_c \to 0$ in the results with a massive c-quark in the closed fermion loop.

From the results below one can see that the first three orders in the expansion over z already exhibit a good convergence.

Our convention for the loop measure is

$$\int [dk] = \int \frac{dk_1^d}{(2\pi)^d} \int \frac{dk_2^d}{(2\pi)^d} \int \frac{dk_3^d}{(2\pi)^d}. \tag{B.1}$$

Some of the integrals in the following subsections have more than one cut (e.g. 2, 3 and 4 particle cuts). The following subsections quote the results of the various cuts. We write

$$\mathrm{Im} \; = \mathrm{Im}^{\,(2)} + \mathrm{Im}^{\,(3)} + \mathrm{Im}^{\,(4)}$$

to separate the contributions from these cuts.

B.1 Results for the four-particle cuts of the master integrals

$$\begin{aligned}
&\mathrm{Im}^{\,(4)} \int [dk] \frac{1}{(k_2^2-m_b^2)\,k_3^2\,((k_1-p_b)^2-m_c^2)\,((k_1-k_2)^2-m_c^2)\,(k_2-k_3)^2} \\
&= \frac{m_b^{2-6\epsilon}}{8192\pi^5} \left[\frac{2z^7(35\log z+611)}{1225} + \frac{1}{200} z^6 (20\log z+151) + z^5 \left(\frac{\log z}{5} + \frac{559}{900} \right) \right. \\
&\quad + z^4 \left(\frac{\log z}{2} + \frac{7}{24} \right) + z^3 \left(2\log z - \frac{11}{3} \right) + z^2 \left(\log^2 z - 7\log z + \frac{27}{2} \right) \\
&\quad - \frac{2}{3} z \left(6\log z + \pi^2 + 6 \right) + \frac{\pi^2}{3} - \frac{7}{2} \\
&\quad + \epsilon \Big(z^7 (-0.0792168\log z - 1.3829) + z^6 (-0.138629\log z - 1.04665) \\
&\quad + z^5 (-0.277259\log z - 0.861043) + z^4 (4.3\log z - 8.65202) + z^3 (-1.33333\log z - 14.4059) \\
&\quad + z^2 \left(-\log^3 z + 4.5\log^2 z - 11.6595\log z + 33.472 \right) + z \left(2\log^2 z - 32\log z - 102.311 \right) \\
&\quad \left. -3.00788 z^{7/2} - 21.0552 z^{5/2} + 105.276 z^{3/2} - 2.50034 \Big) \right] + \mathcal{O}\left(z^8, \epsilon^2\right),
\end{aligned} \tag{B.2}$$

JHEP10(2017)191

$$
\begin{aligned}
&\mathrm{Im}^{(4)}\int[dk]\frac{1}{\left(k_2^2-m_g^2\right)\left(k_3^2-m_c^2\right)(k_1-p_b)^2(k_1-k_2)^2\left((k_2-k_3)^2-m_c^2\right)}\\
&=\frac{m_b^{2-6\epsilon}}{8192\pi^5}\left[-\frac{2\pi^2 z}{3}+\frac{1}{2}\sqrt{1-4z}(2z-9)+2z\log^2\sigma-8z\mathrm{Li}_2(-\sigma)\right.\\
&\quad+\log\sigma\left(-1-4z-2z^2-8z\log(1-\sigma)+4z\log(1-4z)\right)\\
&\quad+z_g\left(4\mathrm{Li}_2(-\sigma)-2\log\sigma(z+2+\log(1-4z)-2\log(1-\sigma))+\frac{\sqrt{1-4z}(1-58z)}{6z}+\frac{\pi^2}{3}-\log^2\sigma\right)\\
&\quad+z_g^2\left(\frac{\sqrt{1-4z}\left(128z^2+166z+3\right)}{180z^2}+\left(\frac{1}{3z}+1\right)\log\sigma\right)\\
&\quad\left.+z_g^3\left(\frac{\sqrt{1-4z}(384z^3-512z^2+464z+15)}{6300z^3}+\frac{\log\sigma}{30z^2}\right)\right]+\mathcal{O}\left(z_g^4,\epsilon^1\right),
\end{aligned}
\tag{B.3}
$$

$$
\begin{aligned}
&\mathrm{Im}^{(4)}\int[dk]\frac{1}{(k_3^2-m_c^2)(k_1-p_b)^2(k_1-k_2)^2\left((k_2-k_3)^2-m_c^2\right)}\\
&=\frac{m_b^{4-6\epsilon}}{49152\pi^5}\left[-48z^2\mathrm{Li}_2(-\sigma)+12z^2\log\sigma(2\log(1-4z)-4\log(1-\sigma)+\log\sigma)\right.\\
&\quad\left.-4\pi^2z^2+\sqrt{1-4z}\left(12z^2+20z+1\right)+12(1-z)(2z+1)z\log\sigma\right]+\mathcal{O}\left(\epsilon^1\right),
\end{aligned}
\tag{B.4}
$$

$$
\begin{aligned}
&\mathrm{Im}^{(4)}\int[dk]\frac{1}{\left(k_2^2-m_g^2\right)\left(k_3^2-m_c^2\right)(k_1-p_b)^2\left((k_2-p_b)^2-m_b^2\right)(k_1-k_2)^2\left((k_2-k_3)^2-m_c^2\right)}\\
&=\frac{m_b^{-6\epsilon}}{8192\pi^5}\left[z^6\left(\frac{\log z}{55}+\frac{958}{3025}\right)+z^5\left(\frac{\log z}{30}+\frac{1349}{5400}\right)+z^4\left(\frac{\log z}{14}+\frac{761}{3528}\right)\right.\\
&\quad+z^3\left(\frac{\log z}{5}+\frac{13}{150}\right)+z^2\left(\log z-\frac{13}{6}\right)+z\left(\log^2 z-10\log z+30\right)-4\pi^2\sqrt{z}+2\log z+\frac{\pi^2}{3}+8\\
&\quad+z_g\left(z^6\left(\frac{\log z}{286}+\frac{90943}{613470}\right)+z^5\left(\frac{\log z}{165}+\frac{17189}{163350}\right)+z^4\left(\frac{\log z}{84}+\frac{1867}{21168}\right)+z^3\left(\frac{\log z}{35}+\frac{904}{11025}\right)\right.\\
&\quad+\frac{1}{100}z^2(10\log z+1)+z\left(\log z-\frac{11}{3}\right)+\frac{\pi^2\sqrt{z}}{2}-\frac{\log^2 z}{2}+2\log z-6+\frac{\pi^2}{2\sqrt{z}}-\frac{1}{3z}\Big)\\
&\quad+z_g^2\left(\frac{\pi^2}{32z^{3/2}}+z^6\left(\frac{\log z}{1430}+\frac{3319103}{42942900}\right)+z^5\left(\frac{\log z}{858}+\frac{544943}{11042460}\right)+z^4\left(\frac{\log z}{462}+\frac{119729}{3201660}\right)\right.\\
&\quad+z^3\left(\frac{\log z}{210}+\frac{4573}{132300}\right)+z^2\left(\frac{\log z}{70}+\frac{799}{22050}\right)+\frac{z}{50}(5\log z-7)+\frac{\pi^2\sqrt{z}}{32}+\frac{1}{6}(2-3\log z)\\
&\quad\left.\left.-\frac{\pi^2}{16\sqrt{z}}+\frac{3\log z-4}{18z}-\frac{1}{30z^2}\right)\right]+\mathcal{O}\left(z^7,z_g^3,\epsilon^1\right),
\end{aligned}
\tag{B.5}
$$

$$
\begin{aligned}
&\mathrm{Im}^{(4)}\int[dk]\frac{1}{k_1^2(k_1-p_b)^2\left((k_2-p_b)^2-m_b^2\right)(k_1-k_2)^2\left(k_3^2-m_c^2\right)\left((k_2-k_3)^2-m_c^2\right)}\\
&=\frac{m_b^{-6\epsilon}}{8192\pi^5}\left[z^5(0.075\log z+0.385)+z^4(0.166667\log z+0.310185)+z^3(0.5\log z-0.166667)\right.\\
&\quad\left.+z^2(3\log z-9.5)+z\left(-0.333333\log^3 z+\log^2 z+4.57974\log z+9.84495\right)-0.710132\right]\\
&\quad+\mathcal{O}\left(z^6,\epsilon^1\right),
\end{aligned}
\tag{B.6}
$$

$$
\begin{aligned}
&\mathrm{Im}^{(4)}\int[dk]\frac{1}{k_1^2k_2^2(k_1-p_b)^2(k_2-p_b)^2\left((k_1-k_3)^2-m_c^2\right)\left((k_2-k_3)^2-m_c^2\right)}\\
&=\frac{m_b^{-6\epsilon}}{2048\pi^5}\left[z^7\left(\log z\left(44\log z+\frac{27634}{315}\right)-22\pi^2-\frac{209379}{1225}\right)+\frac{1}{6}\left(\pi^2-6\right)\right.\\
&\quad+z^6\left(-\log z\left(\frac{84\log z}{5}+\frac{466}{15}\right)+\frac{42\pi^2}{5}+\frac{75343}{1125}\right)+z^5\left(\log z\left(7\log(z)+\frac{172}{15}\right)-\frac{7\pi^2}{2}-\frac{104551}{3600}\right)
\end{aligned}
$$

JHEP10(2017)191

$$+z^4\left(-\log z\left(\frac{10\log z}{3}+\frac{13}{3}\right)+\frac{5\pi^2}{3}+\frac{511}{36}\right)+z^3\left(\log z\left(2\log z+\frac{4}{3}\right)-\pi^2-\frac{161}{18}\right)$$
$$+z^2\left(2(1-\log z)\log z+\pi^2+5\right)+\frac{1}{3}z\left(\log z\left((\log z-3)\log z-2\pi^2+6\right)-30\zeta(3)+2\pi^2-6\right)\Big]$$
$$+\mathcal{O}\left(z^8,\epsilon^1\right), \tag{B.7}$$

$$\mathrm{Im}^{(4)}\int[dk]\frac{(k_3.p_b)}{(k_3^2-m_c^2)(k_1-p_b)^2(k_1-k_2)^2\left((k_2-k_3)^2-m_c^2\right)}$$
$$=\frac{m_b^{6-6\epsilon}}{49152\pi^5}\Big[2z\left(-5z^3+6z^2-3z+1\right)\log\sigma+\frac{1}{12}\sqrt{1-4z}\left(60z^3-62z^2+26z+3\right)$$
$$+\epsilon\left(\frac{71}{24}+z^8\left(-\frac{858\log z}{35}-\frac{570523}{7350}\right)+z^7\left(-\frac{88\log z}{5}-\frac{70991}{1575}\right)+z^6\left(-\frac{84\log z}{5}-\frac{8177}{300}\right)\right.$$
$$+z^5\left(\frac{541}{60}-28\log z\right)+z^4\left(-\frac{67\log z}{3}+\frac{35\pi^2}{3}+\frac{737}{12}\right)+z^3\left(62\log z-14\pi^2+\frac{91}{3}\right)$$
$$\left.+z^2\left(3\log^2 z-36\log z+6\pi^2-\frac{105}{2}\right)+z\left(-\log^2 z+15\log z-2\pi^2+\frac{427}{18}\right)\right)\Big]$$
$$+\mathcal{O}\left(z^9,\epsilon^2\right), \tag{B.8}$$

$$\mathrm{Im}^{(4)}\int[dk]\frac{k_1^2}{k_2^2(k_1-p_b)^2\left((k_1-k_3)^2-m_c^2\right)\left((k_2-k_3)^2-m_c^2\right)}$$
$$=\frac{m_b^{6-6\epsilon}}{294912\pi^5}\left(24z\left(-5z^3+6z^2-3z+1\right)\log\sigma+\sqrt{1-4z}\left(60z^3-62z^2+26z+3\right)\right)$$
$$+\mathcal{O}\left(\epsilon^1\right). \tag{B.9}$$

B.2 Results for the three-particle cuts of the master integrals

$$\mathrm{Im}^{(3)}\int[dk]\frac{1}{(p_b-k_1)^2(k_1-k_2)^2k_2^2(k_3^2-m_c^2)} \tag{B.10}$$
$$=\frac{m_b^{4-6\epsilon}z}{8192\pi^5}\left[-\frac{1}{\epsilon}+\log z-\frac{15}{2}+\frac{1}{4}\epsilon\left(30\log z-2\log^2 z+3\pi^2-145\right)\right.$$
$$\left.+\frac{1}{24}\epsilon^2\left(45\left(3\pi^2-77\right)+2\log z\left(\log z(2\log z-45)-9\pi^2+435\right)+264\zeta(3)\right)\right]+\mathcal{O}(\epsilon^3),$$

$$\mathrm{Im}^{(3)}\int[dk]\frac{1}{(p_b-k_1)^2(k_1-k_2)^2(k_2^2-m_g^2)(k_3^2-m_c^2)}$$
$$=\frac{m_b^{4-6\epsilon}z}{8192\pi^5}\left[\frac{z_g^2-2z_g\log z_g-1}{\epsilon}+\log z-\frac{15}{2}\right.$$
$$+z_g\left(2\log z_g\left(\log z-4\right)+\log^2 z_g+\frac{4}{3}\left(\pi^2-3\right)\right)$$
$$\left.+z_g^2\left(-\log z+\log z_g-\frac{5}{2}\right)+\frac{2z_g^3}{3}\right]+\mathcal{O}(z_g^4,\epsilon^1), \tag{B.11}$$

$$\mathrm{Im}^{(3)}\int[dk]\frac{1}{(p_b-k_1)^2(k_1-k_2)^2(k_2^2-m_g^2)(k_3^2-m_c^2)\left((p_b-k_2)^2-m_b^2\right)}$$
$$=\frac{m_b^{2-6\epsilon}z}{4096\pi^5}\left[\frac{-2\pi\sqrt{z_g}+z_g(4-\log z_g)+2}{2\epsilon}\right.$$

JHEP10(2017)191

$$
\begin{aligned}
&- \log z + 8 + \pi\sqrt{z_g}\,(\log z + \log(4z_g) - 5) \\
&+ \frac{1}{12} z_g \left(6(\log z_g - 4)\log z + 3(\log z_g - 1)^2 + 4\pi^2 - 15\right)\Big] + \mathcal{O}(z_g^{3/2}, \epsilon^1), \qquad \text{(B.12)}
\end{aligned}
$$

$$
\begin{aligned}
&\mathrm{Im}^{(3)} \int [dk] \frac{1}{(p_b - k_1)^2 (k_1 - k_2)^2 (k_2^2 - m_g^2)(k_3^2 - m_c^2)\left((k_2 - k_3)^2 - m_c^2\right)} \\
&= \frac{m_b^{2-6\epsilon}}{8192\pi^5} \left[\frac{z_g^2 - 2 z_g \log z_g - 1}{\epsilon} - \frac{13}{2} + \log z \right. \\
&+ z_g \left(2\log z_g\,(\log z - 3) - \frac{1}{6z} + \log^2 z_g + \frac{4}{3}\left(\pi^2 - 3\right)\right) \\
&\left. + z_g^2 \left(-\frac{(1-3z)\log z_g}{3z} - \log z - \frac{1}{60 z^2} - \frac{7}{2}\right)\right] + \mathcal{O}(z_g^3, \epsilon^1), \qquad \text{(B.13)}
\end{aligned}
$$

$$
\begin{aligned}
&\mathrm{Im}^{(3)} \int [dk] \frac{1}{\left(k_2^2 - m_g^2\right)\left(k_3^2 - m_c^2\right)(k_1 - p_b)^2 \left((k_2 - p_b)^2 - m_b^2\right)(k_1 - k_2)^2 \left((k_2 - k_3)^2 - m_c^2\right)} \\
&= \frac{m_b^{-6\epsilon}}{4096\pi^5} \left[\frac{-2\pi\sqrt{z_g} + z_g(4 - \log z_g) + 2}{2\epsilon}\right. \\
&- \log z + 7 + \pi\sqrt{z_g}\,(\log z + \log(4z_g) - 4) \\
&\left. + \frac{1}{12} z_g \left(6(\log z_g - 4)\log z + 3\log^2 z_g + 4\pi^2 - 36 + \frac{2}{z}\right)\right] + \mathcal{O}(z_g^{3/2}, \epsilon^1), \qquad \text{(B.14)}
\end{aligned}
$$

B.3 Results for the two-particle cuts of the master integrals

$$
\begin{aligned}
&\mathrm{Im}^{(2)} \int [dk] \frac{1}{k_1^2 k_2^2 (k_1 - p_b)^2 (k_2 - p_b)^2 \left((k_1 - k_3)^2 - m_c^2\right)\left((k_2 - k_3)^2 - m_c^2\right)} \\
&= \frac{m_b^{-6\epsilon}}{8192\pi^5} \left[\frac{2}{\epsilon^2} + \frac{14}{\epsilon} - z^8 \left(\frac{1144}{7}\pi^2 + \frac{324314461}{617400} - \frac{54031}{105}\log z - \frac{1716}{7}\log^2 z\right)\right. \\
&+ z^7 \left(\frac{176\pi^2}{3} + \frac{2168531}{11025} - \frac{55268}{315}\log z - 88\log^2 z\right) - z^6 \left(\frac{112\pi^2}{5} + \frac{88799}{1125} - \frac{932}{15}\log z - \frac{168}{5}\log^2 z\right) \\
&+ z^5 \left(\frac{28\pi^2}{3} + \frac{31363}{900} - \frac{344}{15}\log z - 14\log^2 z\right) - z^4 \left(\frac{40\pi^2}{9} + \frac{953}{54} - \frac{26}{3}\log z - \frac{20}{3}\log^2 z\right) \\
&+ z^3 \left(\frac{8\pi^2}{3} + \frac{98}{9} - \frac{8}{3}\log z - 4\log^2 z\right) - z^2 \left(\frac{8\pi^2}{3} + 6 + 4\log z - 4\log^2 z\right) \\
&\left. + z \left(16\zeta(3) - \frac{8\pi^2}{3} + 8 + 8\left(\frac{\pi^2}{3} - 1\right)\log z + 4\log^2 z - \frac{4}{3}\log^3 z\right) - \frac{25\pi^2}{6} + 66\right] + \mathcal{O}(z^9, \epsilon^1), \qquad \text{(B.15)}
\end{aligned}
$$

$$
\begin{aligned}
&\mathrm{Im}^{(2)} \int [dk] \frac{1}{k_1^2 (k_1 - p_b)^2 (k_3^2 - m_c^2)\left((k_2 - p_b)^2 - m_b^2\right)\left((k_2 - k_3)^2 - m_c^2\right)} \\
&= \frac{m_b^{2-6\epsilon}}{8192\pi^5} \left[\frac{-2z - 1}{\epsilon^2} + \frac{2z\,(2\log z - 5) - \frac{9}{2}}{\epsilon} + z^8 \left(\frac{73}{14112} - \frac{\log z}{84}\right)\right. \\
&+ z^7 \left(\frac{107}{11025} - \frac{2}{105}\log z\right) + z^6 \left(\frac{37}{1800} - \frac{\log z}{30}\right) + z^5 \left(\frac{47}{900} - \frac{\log z}{15}\right) \\
&+ z^4 \left(\frac{13}{72} - \frac{\log z}{6}\right) + z^3 \left(\frac{11}{9} - \frac{2}{3}\log z\right) + z^2 \left(-\frac{2\pi^2}{3} - \frac{7}{2} + 3\log z - \log^2 z\right) \\
&\left. + z \left(\frac{3\pi^2}{2} - 30 + 20\log z - 2\log^2 z\right) - \frac{7\pi^2}{12} - \frac{47}{4}\right] + \mathcal{O}(z^9, \epsilon^1), \qquad \text{(B.16)}
\end{aligned}
$$

JHEP10(2017)191

$$\begin{aligned}
&\mathrm{Im}^{(2)}\int[dk]\frac{1}{k_1^2(k_1-p)^2(k_2^2-m_g^2)(k_3^2-m_c^2)\left((k_2-p_b)^2-m_b^2\right)\left((k_2-k_3)^2-m_c^2\right)}\\
&=\frac{m_b^{-6\epsilon}}{8192\pi^5}\left[-\frac{1}{\epsilon^2}+\frac{2\pi\sqrt{z_g}+z_g(\log z_g-2)-7}{\epsilon}+z^6\left(\frac{181}{54450}-\frac{\log z}{165}\right)\right.\\
&+z^5\left(\frac{121}{16200}-\frac{\log z}{90}\right)+z^4\left(\frac{73}{3528}-\frac{\log z}{42}\right)+z^3\left(\frac{37}{450}-\frac{\log z}{15}\right)+z^2\left(\frac{13}{18}-\frac{1}{3}\log z\right)\\
&\left.+4\pi^2\sqrt{z}+z\left(-\frac{2\pi^2}{3}-14+6\log z-\log^2 z\right)-\frac{7\pi^2}{12}-33\right]+\mathcal{O}(z^7,\epsilon^1),
\end{aligned}\tag{B.17}$$

$$\begin{aligned}
&\mathrm{Im}^{(2)}\int[dk]\frac{1}{k_1^2(k_1-p_b)^2(k_2^2-m_g^2)(k_3^2-m_c^2)\left((k_2-k_3)^2-m_c^2\right)}\\
&=\frac{m_b^{2-6\epsilon}}{8192\pi^5}\left[\frac{-2z-z_g}{\epsilon^2}+\frac{2z(2\log z-5)+z_g(2\log z_g-5)}{\epsilon}\right.\\
&+\frac{1}{6}z\left(-24\log^2 z+120\log z+\pi^2-204\right)\\
&\left.+z_g\left(-2\log z(\log z_g-2)+\log^2 z-\log^2 z_g+6\log z_g+\frac{\pi^2}{12}-9\right)\right]+\mathcal{O}(z_g^2,\epsilon^1),
\end{aligned}\tag{B.18}$$

$$\begin{aligned}
&\mathrm{Im}^{(2)}\int[dk]\frac{1}{k_1^2(k_1-p_b)^2(k_2^2-m_g^2)\left((k_2-p_b)^2-m_b^2\right)(k_3^2-m_c^2)}\\
&=\frac{m_b^{2-6\epsilon}z}{8192\pi^5}\left[-\frac{2}{\epsilon^2}+\frac{2(\log z-5)-\frac{1}{4}\pi z_g^{3/2}+\frac{z_g^2}{6}+2\pi\sqrt{z_g}+z_g(\log z_g-2)}{\epsilon}\right.\\
&-\log^2 z+10\log z+\frac{\pi^2}{6}-34-2\pi\sqrt{z_g}(\log z+\log(4z_g)-5)\\
&+\frac{1}{2}z_g\left(-2\log z\log z_g+4\log z-\log^2 z_g+6\log z_g-4\right)+\frac{1}{4}\pi z_g^{3/2}(\log z+\log(4z_g)-3)\\
&\left.+\frac{1}{6}z_g^2(-\log z-3\log(4z_g)+19-\log 4)\right]+\mathcal{O}(z_g^{5/2},\epsilon^1),
\end{aligned}\tag{B.19}$$

$$\begin{aligned}
&\mathrm{Im}^{(2)}\int[dk]\frac{1}{k_1^2(k_1-p_b)^2(k_3^2-m_c^2)\left((k_2-p_b)^2-m_b^2\right)\left((k_2-k_3)^2-m_c^2\right)}\\
&=\frac{m_b^{2-6\epsilon}}{4096\pi^5}\left[\frac{z+\frac{1}{2}}{\epsilon^2}+\frac{z(5-2\log z)+\frac{9}{4}}{\epsilon}+z^8\left(\frac{\log z}{168}-\frac{1}{28224}73\right)+z^7\left(\frac{\log z}{105}-\frac{107}{22050}\right)\right.\\
&+z^6\left(\frac{\log z}{60}-\frac{37}{3600}\right)+z^5\left(\frac{\log z}{30}-\frac{47}{1800}\right)+z^4\left(\frac{\log z}{12}-\frac{13}{144}\right)+z^3\left(\frac{\log z}{3}-\frac{11}{18}\right)\\
&+z^2\left(\frac{\log^2 z}{2}-\frac{3}{2}\log z+\frac{\pi^2}{3}+\frac{7}{4}\right)+z\left(\log^2 z-10\log z-\frac{3\pi^2}{4}+15\right)+\frac{7\pi^2}{24}+\frac{47}{8}\\
&+\epsilon\left(-\frac{16}{315}\pi^2 z^{9/2}-\frac{16}{105}\pi^2 z^{7/2}-\frac{16}{15}\pi^2 z^{5/2}+\frac{16}{3}\pi^2 z^{3/2}-\frac{16\pi^2 z^{15/2}}{2145}-\frac{16\pi^2 z^{13/2}}{1287}-\frac{16}{693}\pi^2 z^{11/2}\right.\\
&+z^8\left(\frac{890041\log z}{30270240}+\frac{\pi^2}{168}-\frac{113307356143}{10908183686400}\right)+z^7\left(\frac{62281\log z}{1455300}+\frac{\pi^2}{105}-\frac{344223461}{20170458000}\right)\\
&+z^6\left(\frac{2473\log z}{37800}+\frac{\pi^2}{60}-\frac{1403863}{47628000}\right)+z^5\left(\frac{661}{6300}\log z+\frac{\pi^2}{30}-\frac{44969}{882000}\right)\\
&+z^4\left(\frac{29}{180}\log z+\frac{\pi^2}{12}-\frac{49}{1200}\right)+z^3\left(\frac{\pi^2}{3}+\frac{17}{9}-\frac{2}{9}\log z\right)\\
&\left.+\frac{1}{8}z^2\left(-4\log^3 z+18\log^2 z-10\log z+32\zeta(3)-67\right)\right.
\end{aligned}$$

JHEP10(2017)191

$$+z\left(-\frac{1}{3}\log^3 z+5\log^2 z+\left(\frac{\pi^2}{6}-34\right)\log z-11\zeta(3)-\frac{15\pi^2}{4}+33\right)$$
$$+\frac{5}{2}\zeta(3)+\frac{133}{16}+\frac{21\pi^2}{16}\Bigg)\Bigg]+\mathcal{O}(z^9,\epsilon^2), \tag{B.20}$$

$$\begin{aligned}&\mathrm{Im}^{(2)}\int[dk]\frac{1}{k_1^2(k_1-p_b)^2k_2^2(k_2-p_b)^2(k_3^2-m_c^2)\left((k_3-p_b)^2-m_c^2\right)}\\&=\frac{m_b^{-6\epsilon}}{4096\pi^5}\Bigg[\frac{\sqrt{1-4z}+2}{\epsilon^2}+\frac{\sqrt{1-4z}(2\log\sigma-\log(1-4z)+6)-2\log z+12}{\epsilon}\\&\quad+\log^2 z-12\log z-\frac{3\pi^2}{2}+48+\sqrt{1-4z}\left(4\mathrm{Li}_2\left(\frac{1}{2}-\frac{1}{2\sqrt{1-4z}}\right)-\frac{\log^2\sigma}{2}+12\log\sigma\right.\\&\quad\left.-\log(1-4z)(\log\sigma+\log z+4)-\log\sigma\log z+\frac{1}{2}\log^2(1-4z)+\frac{\log^2 z}{2}-\frac{7\pi^2}{2}+20\right)\Bigg]\\&\quad+\mathcal{O}(\epsilon^1).\end{aligned} \tag{B.21}$$

B.4 Results for integrals with a *b* quark

The master integrals with a heavy b quark have only one cut which contributes to the imaginary part.

$$\begin{aligned}&\mathrm{Im}\int[dk]\frac{1}{(p_b-k_1)^2(k_1-k_2)^2(k_2^2-m_g^2)(k_3^2-m_b^2)\left((k_2-k_3)^2-m_b^2\right)}\\&=\frac{m_b^{2-6\epsilon}}{2(4\pi)^5}\left[\frac{\frac{{z_g}^2}{4}-\frac{1}{2}z_g\log z_g-\frac{1}{4}}{\epsilon}+{z_g}^2\left(\frac{\log z_g}{6}-\frac{211}{240}\right)\right.\\&\quad\left.+\frac{1}{24}z_g\left(6\log^2 z_g-36\log z_g+8\pi^2-25\right)-\frac{13}{8}\right]+\mathcal{O}\left(z_g^3,\epsilon^1\right),\end{aligned} \tag{B.22}$$

$$\begin{aligned}&\mathrm{Im}\int[dk]\frac{1}{(p_b-k_1)^2(k_1-k_2)^2(k_2^2-m_g^2)(k_3^2-m_b^2)((k_2-k_3)^2-m_b^2)\left((p_b-k_2)^2-m_b^2\right)}\\&=\frac{m_b^{-6\epsilon}}{2(4\pi)^5}\left[\frac{-\frac{\pi\sqrt{z_g}}{2}+z_g\left(1-\frac{\log z_g}{4}\right)+\frac{1}{2}}{\epsilon}+\frac{7}{2}\right.\\&\quad\left.+\frac{1}{24}z_g\left(3\log^2 z_g+4\pi^2-34\right)+\frac{1}{2}\pi\sqrt{z_g}(\log z_g-4+\log 4)\right]+\mathcal{O}\left(z_g^{3/2},\epsilon^1\right),\end{aligned} \tag{B.23}$$

$$\begin{aligned}&\mathrm{Im}\int[dk]\frac{1}{(p_b-k_1)^2k_1^2(k_2^2-m_g^2)(k_3^2-m_b^2)\left((k_2-k_3)^2-m_b^2\right)}\\&=\frac{m_b^{2-6\epsilon}}{2(4\pi)^5}\left[\frac{\frac{z_g}{4}+\frac{1}{2}}{\epsilon^2}+\frac{\frac{1}{4}z_g(5-2\log z_g)+\frac{5}{2}}{\epsilon}+\frac{1}{24}\left(204-\pi^2\right)\right.\\&\quad\left.+\frac{1}{48}z_g\left(12\log^2 z_g-72\log z_g-\pi^2+108\right)\right]+\mathcal{O}\left(z_g^2,\epsilon^1\right),\end{aligned} \tag{B.24}$$

JHEP10(2017)191

$$\begin{aligned}
&\mathrm{Im}\int[dk]\frac{1}{(p_b-k_1)^2k_1^2(k_2^2-m_g^2)(k_3^2-m_b^2)\left((k_2-k_3)^2-m_b^2\right)\left((p_b-k_2)^2-m_b^2\right)}\\
&=\frac{m_b^{-6\epsilon}}{2(4\pi)^5}\left[\frac{1}{4\epsilon^2}+\frac{-\frac{\pi\sqrt{z_g}}{2}+\frac{1}{4}z_g(2-\log z_g)+\frac{7}{4}}{\epsilon}-\frac{17\pi^2}{48}+\frac{33}{4}\right.\\
&\left.-\pi\sqrt{z_g}+z_g\left(1-\frac{\log z_g}{2}\right)\right]+\mathcal{O}\left(z_g^{3/2},\epsilon^1\right), \qquad \text{(B.25)}\\
&\mathrm{Im}\int[dk]\frac{1}{(p_b-k_1)^2k_1^2(k_3^2-m_b^2)\left((k_2-k_3)^2-m_b^2\right)\left((p_b-k_2)^2-m_b^2\right)} \qquad \text{(B.26)}\\
&=\frac{m_b^{2-6\epsilon}}{2(4\pi)^5}\left[\frac{3}{4\epsilon^2}+\frac{29}{8\epsilon}+\frac{1}{16}\left(175-\pi^2\right)+\epsilon\left(\frac{765}{32}-\frac{9}{4}\zeta(3)+\frac{35\pi^2}{96}\right)\right]+\mathcal{O}(\epsilon^2),\\
&\mathrm{Im}\int[dk]\frac{1}{(p_b-k_1)^2k_1^2(k_1-k_2)^2(k_3^2-m_b^2)\left((k_2-k_3)^2-m_b^2\right)\left((p_b-k_2)^2-m_b^2\right)} \qquad \text{(B.27)}\\
&=\frac{m_b^{-6\epsilon}}{2(4\pi)^5}\left[\frac{1}{\epsilon^2}+\frac{5}{\epsilon}-\frac{\pi^2}{12}-4\zeta(3)+15\right]+\mathcal{O}(\epsilon^1),\\
&\mathrm{Im}\int[dk]\frac{1}{(p_b-k_1)^2k_1^2(p_b-k_2)^2k_2^2\left((k_2-k_3)^2-m_b^2\right)\left((k_1-k_3)^2-m_b^2\right)} \qquad \text{(B.28)}\\
&=\frac{m_b^{-6\epsilon}}{2(4\pi)^5}\left[\frac{1}{2\epsilon^2}+\frac{7}{2\epsilon}+\frac{33}{2}+\pi^2\left(-\frac{17}{24}-\frac{1}{\sqrt{5}}-\frac{4}{5}\log\frac{1+\sqrt{5}}{2}\right)+\frac{4\zeta(3)}{5}\right]+\mathcal{O}(\epsilon^1),\\
&\mathrm{Im}\int[dk]\frac{k_3^2}{(p_b-k_1)^2k_1^2(p_b-k_2)^2k_2^2\left((k_2-k_3)^2-m_b^2\right)\left((k_1-k_3)^2-m_b^2\right)} \qquad \text{(B.29)}\\
&=\frac{m_b^{2-6\epsilon}}{2(4\pi)^5}\left[\frac{13}{8\epsilon^2}+\frac{149}{16\epsilon}+\frac{1203}{32}-\pi^2\left(\frac{157}{96}+\frac{7}{4\sqrt{5}}+\frac{2}{5}\log\frac{1+\sqrt{5}}{2}\right)+\frac{2\zeta(3)}{5}\right]+\mathcal{O}(\epsilon^1).
\end{aligned}$$

References

[1] HFLAV Group, *Summer 2017 averages*, http://www.slac.stanford.edu/xorg/hfag/osc/summer_2017.

[2] CDF collaboration, A. Abulencia et al., *Observation of $B_s^0 - \bar{B}_s^0$ Oscillations*, *Phys. Rev. Lett.* **97** (2006) 242003 [hep-ex/0609040] [INSPIRE].

[3] LHCb collaboration, *Precision measurement of the B_s^0-$\bar{B}_s^0$ oscillation frequency with the decay $B_s^0 \to D_s^- \pi^+$*, *New J. Phys.* **15** (2013) 053021 [arXiv:1304.4741] [INSPIRE].

[4] LHCb collaboration, *Precision measurement of CP violation in $B_s^0 \to J/\psi K^+ K^-$ decays*, *Phys. Rev. Lett.* **114** (2015) 041801 [arXiv:1411.3104] [INSPIRE].

[5] LHCb collaboration, *First study of the CP-violating phase and decay-width difference in $B_s^0 \to \psi(2S)\phi$ decays*, *Phys. Lett.* **B 762** (2016) 253 [arXiv:1608.04855] [INSPIRE].

JHEP10(2017)191

[6] ATLAS collaboration, *Measurement of the CP-violating phase ϕ_s and the B_s^0 meson decay width difference with $B_s^0 \to J/\psi\phi$ decays in ATLAS*, *JHEP* **08** (2016) 147 [arXiv:1601.03297] [INSPIRE].

[7] CMS collaboration, *Measurement of the CP-violating weak phase ϕ_s and the decay width difference $\Delta\Gamma_s$ using the $B_s^0 \to J/\psi\phi(1020)$ decay channel in pp collisions at $\sqrt{s} = 8$ TeV*, *Phys. Lett.* **B 757** (2016) 97 [arXiv:1507.07527] [INSPIRE].

[8] CDF collaboration, T. Aaltonen et al., *Measurement of the Bottom-Strange Meson Mixing Phase in the Full CDF Data Set*, *Phys. Rev. Lett.* **109** (2012) 171802 [arXiv:1208.2967] [INSPIRE].

[9] M. Beneke, G. Buchalla, A. Lenz and U. Nierste, *CP asymmetry in flavor specific B decays beyond leading logarithms*, *Phys. Lett.* **B 576** (2003) 173 [hep-ph/0307344] [INSPIRE].

[10] A. Lenz and U. Nierste, *Theoretical update of $B_s - \bar{B}_s$ mixing*, *JHEP* **06** (2007) 072 [hep-ph/0612167] [INSPIRE].

[11] A. Lenz and U. Nierste, *Numerical Updates of Lifetimes and Mixing Parameters of B Mesons*, arXiv:1102.4274 [INSPIRE].

[12] U. Nierste, *B Mixing in the Standard Model and Beyond*, arXiv:1212.5805 [INSPIRE].

[13] V.A. Khoze and M.A. Shifman, *Heavy Quarks*, *Sov. Phys. Usp.* **26** (1983) 387 [INSPIRE].

[14] M.A. Shifman and M.B. Voloshin, *Preasymptotic Effects in Inclusive Weak Decays of Charmed Particles*, *Sov. J. Nucl. Phys.* **41** (1985) 120 [INSPIRE].

[15] M.A. Shifman and M.B. Voloshin, *Hierarchy of Lifetimes of Charmed and Beautiful Hadrons*, *Sov. Phys. JETP* **64** (1986) 698 [INSPIRE].

[16] I.I.Y. Bigi, N.G. Uraltsev and A.I. Vainshtein, *Nonperturbative corrections to inclusive beauty and charm decays: QCD versus phenomenological models*, *Phys. Lett.* **B 293** (1992) 430 [*Erratum ibid.* **B 297** (1992) 477] [hep-ph/9207214] [INSPIRE].

[17] M. Beneke, G. Buchalla and I. Dunietz, *Width Difference in the $B_s - \bar{B}_s$ System*, *Phys. Rev.* **D 54** (1996) 4419 [*Erratum ibid.* **D 83** (2011) 119902] [hep-ph/9605259] [INSPIRE].

[18] M. Beneke, G. Buchalla, C. Greub, A. Lenz and U. Nierste, *Next-to-leading order QCD corrections to the lifetime difference of B(s) mesons*, *Phys. Lett.* **B 459** (1999) 631 [hep-ph/9808385] [INSPIRE].

[19] M. Ciuchini, E. Franco, V. Lubicz, F. Mescia and C. Tarantino, *Lifetime differences and CP-violation parameters of neutral B mesons at the next-to-leading order in QCD*, *JHEP* **08** (2003) 031 [hep-ph/0308029] [INSPIRE].

[20] Fermilab Lattice, MILC collaborations, A. Bazavov et al., *$B^0_{(s)}$-mixing matrix elements from lattice QCD for the Standard Model and beyond*, *Phys. Rev.* **D 93** (2016) 113016 [arXiv:1602.03560] [INSPIRE].

[21] A. Badin, F. Gabbiani and A.A. Petrov, *Lifetime difference in B_s mixing: Standard model and beyond*, *Phys. Lett.* **B 653** (2007) 230 [arXiv:0707.0294] [INSPIRE].

[22] G. Buchalla, A.J. Buras and M.E. Lautenbacher, *Weak decays beyond leading logarithms*, *Rev. Mod. Phys.* **68** (1996) 1125 [hep-ph/9512380] [INSPIRE].

[23] M. Gorbahn and U. Haisch, *Effective Hamiltonian for non-leptonic $|\Delta F| = 1$ decays at NNLO in QCD*, *Nucl. Phys.* **B 713** (2005) 291 [hep-ph/0411071] [INSPIRE].

JHEP10(2017)191

[24] M. Gorbahn, U. Haisch and M. Misiak, *Three-loop mixing of dipole operators*, *Phys. Rev. Lett.* **95** (2005) 102004 [hep-ph/0504194] [INSPIRE].

[25] S.J. Brodsky, G.P. Lepage and P.B. Mackenzie, *On the Elimination of Scale Ambiguities in Perturbative Quantum Chromodynamics*, *Phys. Rev.* **D 28** (1983) 228 [INSPIRE].

[26] M. Beneke and V.M. Braun, *Naive nonAbelianization and resummation of fermion bubble chains*, *Phys. Lett.* **B 348** (1995) 513 [hep-ph/9411229] [INSPIRE].

[27] H.M. Asatrian, T. Ewerth, A. Ferroglia, C. Greub and G. Ossola, *Complete* (O_7, O_8) *contribution to* $B \to X_s\gamma$ *at order* α_s^2, *Phys. Rev.* **D 82** (2010) 074006 [arXiv:1005.5587] [INSPIRE].

[28] M. Beneke, G. Buchalla, C. Greub, A. Lenz and U. Nierste, *The* $B^+ - B_d^0$ *lifetime difference beyond leading logarithms*, *Nucl. Phys.* **B 639** (2002) 389 [hep-ph/0202106] [INSPIRE].

[29] A.J. Buras, M. Gorbahn, U. Haisch and U. Nierste, *Charm quark contribution to* $K^+ \to \pi^+\nu\bar{\nu}$ *at next-to-next-to-leading order*, *JHEP* **11** (2006) 002 [*Erratum ibid.* **11** (2012) 167] [hep-ph/0603079] [INSPIRE].

[30] S. Herrlich and U. Nierste, *Evanescent operators, scheme dependences and double insertions*, *Nucl. Phys.* **B 455** (1995) 39 [hep-ph/9412375] [INSPIRE].

[31] K.G. Chetyrkin, M. Misiak and M. Münz, *β-functions and anomalous dimensions up to three loops*, *Nucl. Phys.* **B 518** (1998) 473 [hep-ph/9711266] [INSPIRE].

[32] K. Bieri, C. Greub and M. Steinhauser, *Fermionic NNLL corrections to* $b \to s\gamma$, *Phys. Rev.* **D 67** (2003) 114019 [hep-ph/0302051] [INSPIRE].

[33] A.J. Buras and P.H. Weisz, *QCD Nonleading Corrections to Weak Decays in Dimensional Regularization and 't Hooft-Veltman Schemes*, *Nucl. Phys.* **B 333** (1990) 66 [INSPIRE].

[34] N. Gray, D.J. Broadhurst, W. Grafe and K. Schilcher, *Three loop relation of quark* $\overline{MS}$ *and pole masses*, *Z. Phys.* **C 48** (1990) 673 [INSPIRE].

[35] K.G. Chetyrkin and M. Steinhauser, *The Relation between the MS-bar and the on-shell quark mass at order* α_s^3, *Nucl. Phys.* **B 573** (2000) 617 [hep-ph/9911434] [INSPIRE].

[36] H.M. Asatrian, T. Ewerth, H. Gabrielyan and C. Greub, *Charm quark mass dependence of the electromagnetic dipole operator contribution to* $\bar{B} \to X_s\gamma$ *at* $O(\alpha_s^2)$, *Phys. Lett.* **B 647** (2007) 173 [hep-ph/0611123] [INSPIRE].

[37] Particle Data Group collaboration, C. Patrignani et al., *Review of Particle Physics*, *Chin. Phys.* **C 40** (2016) 100001 [INSPIRE].

[38] CKMfitter Group collaboration, J. Charles et al., *CP violation and the CKM matrix: Assessing the impact of the asymmetric B factories*, *Eur. Phys. J.* **C 41** (2005) 1 [hep-ph/0406184] [INSPIRE].

[39] J.H. Kuhn, M. Steinhauser and C. Sturm, *Heavy Quark Masses from Sum Rules in Four-Loop Approximation*, *Nucl. Phys.* **B 778** (2007) 192 [hep-ph/0702103] [INSPIRE].

[40] HPQCD collaboration, I. Allison et al., *High-Precision Charm-Quark Mass from Current-Current Correlators in Lattice and Continuum QCD*, *Phys. Rev.* **D 78** (2008) 054513 [arXiv:0805.2999] [INSPIRE].

[41] S. Aoki et al., *Review of lattice results concerning low-energy particle physics*, *Eur. Phys. J.* **C 77** (2017) 112 [arXiv:1607.00299] [INSPIRE].

JHEP10(2017)191

[42] T. Huber, E. Lunghi, M. Misiak and D. Wyler, *Electromagnetic logarithms in $\bar{B} \to X_s l^+ l^-$*, *Nucl. Phys.* **B 740** (2006) 105 [hep-ph/0512066] [INSPIRE].

[43] A.V. Smirnov, *Algorithm FIRE — Feynman Integral REduction*, *JHEP* **10** (2008) 107 [arXiv:0807.3243] [INSPIRE].

[44] H.M. Asatrian, A. Hovhannisyan and A. Yeghiazaryan, *The phase space analysis for three and four massive particles in final states*, *Phys. Rev.* **D 86** (2012) 114023 [arXiv:1210.7939] [INSPIRE].

[45] E.E. Boos and A.I. Davydychev, *A method of evaluating massive Feynman integrals*, *Theor. Math. Phys.* **89** (1991) 1052 [INSPIRE].

[46] S. Borowka, G. Heinrich, S.P. Jones, M. Kerner, J. Schlenk and T. Zirke, *SecDec-3.0: numerical evaluation of multi-scale integrals beyond one loop*, *Comput. Phys. Commun.* **196** (2015) 470 [arXiv:1502.06595] [INSPIRE].

JHEP10(2017)191